Geotech Geol Eng (2025) 43:416
https://doi.org/10.1007/s10706-025-03412-8

ORIGINAL PAPER

Experimental Evaluation of Sleeved Rock Bolts for Corrosion Resistance and Load Transfer Performance in Underground Reinforcement

Adel Mottahedi · Naj Aziz · Alex Remennikov · Ali Mirzaghorbanali · Zhenjun Shan

Received: 4 May 2025 / Accepted: 29 August 2025

Abstract Ground reinforcement using rock bolts is critical for long-term stability in underground excavations, but their effectiveness is highly dependent on their resistance to corrosion. While Corrosion Protection Sleeves (CPS) are widely used to mitigate corrosion in steel rock bolts, their mechanical integrity and influence on the overall system's performance under axial and shear displacement remain unquantified. This study addresses this knowledge gap by conducting a comparative analysis of sleeved versus conventional rock bolts, investigating the influence of the host medium type, and assessing the integrity of the CPS under various loading conditions. The findings revealed that sleeved bolts show a more ductile response in pull-out tests compared to conventional bolts, allowing for greater roof convergence before debonding. This contrasts with conventional bolts, which demonstrate higher initial stiffness and bond strength. It was also found that, during axial loading, the main failure mode was debonding at the grout-CPS interface, which was similar to the previous studies. Furthermore, the study identified a critical shear displacement threshold of around 25 mm, beyond which the CPS shows visible cracking. This finding differs from previous studies that reported higher thresholds. The results also highlighted that the failure mode and load transfer capacity are influenced by the stiffness of the surrounding host medium, a factor that was not assessed sufficiently in the literature. These outcomes have significant implications for the design and maintenance of ground reinforcement systems. They highlight that while CPS enhances corrosion resistance, their mechanical performance is adversely affected by ground deformation. This research provided practical guidance for field engineers, emphasizing the need for a cautious design approach and continuous monitoring of sleeved rock bolts in highly deformable ground conditions. Meanwhile, the results can help engineers establish a guide for inspection routines and replacement strategies to ensure the long-term reliability and safety of underground excavations.

Keywords Sleeved rock bolt · Shear test · Pull-out load · Ground control · Corrosion

A. Mottahedi (✉) · N. Aziz · A. Remennikov · Z. Shan
School of Civil, Mining and Environmental Engineering, University of Wollongong, Wollongong, NSW 2522, Australia
e-mail: adelmotahedi@gmail.com; am3887@uowmail.edu.au

N. Aziz
e-mail: naj@uow.edu.au

A. Remennikov
e-mail: alexrem@uow.edu.au

Z. Shan
e-mail: zshan@uow.edu.au

A. Mirzaghorbanali
School of Civil Engineering and Surveying, University of Southern Queensland, Toowoomba, QLD 4350, Australia
e-mail: Ali.Mirzaghorbanali@unisq.edu.au

Published online: 09 September 2025

Abbreviations

CPS	Corrosion protection sleeve
DEPT	Double embedment pull test
DST	Double shear test
LTC	Load transfer capacity
PVC	Polyvinyl chloride
RPTM	Reverse pull-out test machine
SCC	Stress corrosion cracking
SEPT	Single embedment pull test
SST	Single shear test
UCS	Uniaxial compressive strength
UTL	Ultimate tensile load
L_E	Encapsulation length
w/c	Water-to-cement ratio
K	Pull-out stiffness
P_{max}	Peak pull-out load
$\delta_{P_{max}}$	Displacement at peak pull-out load
S_{max}	Peak shear load
δ_S	Shear displacement
k_H	High (initial) stiffness
k_L	Low stiffness

1 Introduction

Excavating underground structures disturbs the initial stress distribution, often leading to instability in the rock mass due to axial and shear deformations (Wu et al. 2018). Reinforcing the rock during and after excavation is critical, as any collapse can jeopardize personnel and assets, resulting in fatalities and costly rehabilitation efforts (Nourizadeh et al. 2024; Hosseini et al. 2024). Thus, to ensure long-term stability, underground openings must be reinforced to maintain their structural integrity throughout their service life (Moosavi and Bawden 2003; Li et al. 2024). Among various rock reinforcement techniques, fully grouted rock bolting systems have become a widely adopted solution. They enhance the load transfer capacity (LTC) of the surrounding rock near excavation boundaries (Ferrero 1995; Moosavi and Bawden 2003; Mottahedi et al. 2025; Rastegarmanesh et al. 2025). Hence, assessing the performance of rock bolts subjected to various loading modes is essential.

1.1 Mechanical Performance (Tensile/Shear)

Rock bolts are typically subjected to axial, shear, or combined loading conditions, as illustrated in Fig. 1 (Hutchinson and Diederichs 1996). Under axial loading (tension), the force per unit length required to pull the bolt out of the host medium is called pull-out strength (Thirukumaran et al. 2025). In fully grouted bolts, axial loads are transferred via chemical adhesion, mechanical interlocking, and frictional resistance along the bolt-grout interface (Moosavi et al. 2005; Peter et al. 2022). Shear performance is equally critical, especially when induced loads exceed

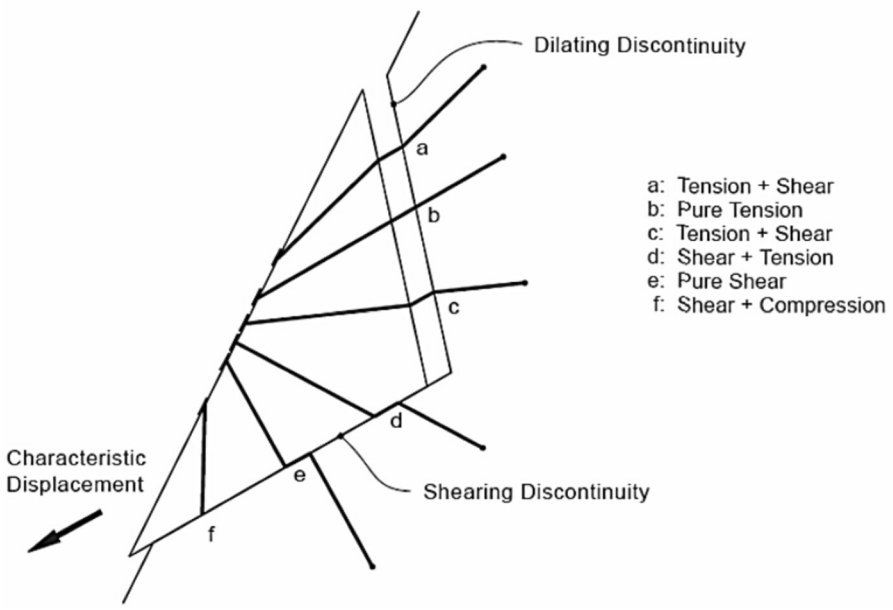

Fig. 1 A schematic view of a rock block reinforced by the rock bolts (thompson et al. 2012)

the shear strength of discontinuities such as bedding planes, joints, and fractures (Knox and Hadjigeorgiou 2022; Jing et al. 2023). Rock bolts enhance frictional strength along these shear planes by compressing the rock mass. After a small displacement, the bolt should reach its maximum shear strength and continue to tolerate further shear displacement without shedding load (Haas 1976; Ludvig 1984; Zheng et al. 2024).

A typical rock bolting system includes a steel rod (element), the surrounding rock mass (host medium), the encapsulation material (e.g., grout/resin), and the external fixtures (e.g., faceplate/nut) (Thompson et al. 2012; Kong et al. 2023). Failure can occur in various components. If the normal or shear stress at the connection point between the rock bolt and faceplate exceeds the rock bolt's strength, failure can occur at that interface. In such cases, the faceplate may detach, allowing the rock bolt to be pulled back into the surrounding rock mass (He et al. 2018; Zhao et al. 2021).

While debonding along the bolt-grout interface is the most common failure mode (Chen et al. 2020), failure may occur along the grout-rock interface in small-diameter boreholes (Cao et al. 2013). Usually, failure takes place along the weakest interface unless the rock bolt itself fails either in shear or tension (Nourizadeh et al. 2024). Therefore, the pull-out and shear capacities of rock bolts primarily depend on the mechanical properties of both the bolt and the encapsulation material, and environmental conditions (e.g., corrosion, temperature) (Høien et al. 2021; Nourizadeh et al. 2023, 2025a; Guo et al. 2025). In this regard, steel rock bolts are highly vulnerable to corrosion, which is a critical factor that can significantly degrade their mechanical properties.

1.2 Corrosion Vulnerability and Mitigation

Corrosion is a major factor that can adversely affect the LTC of rock bolts, especially in underground environments where rock bolts are exposed to groundwater and acidic conditions (Satola and Hakala 2001; Hassell et al. 2006). Corrosion deteriorates the mechanical properties of steel rock bolts and may lead to premature failure of the bolts due to Stress Corrosion Cracking (SCC), which can occur within months or after years of exposure (Wu et al. 2018; Ding et al. 2022a, b). Therefore, long-term installation of rock bolts requires enhanced protection measures.

To mitigate corrosion and improve the life expectancy of rock bolts, effective corrosion protection measures can be implemented. Common measures include coating the steel rock bolt with either cathodic sacrificial layers, such as zinc and zinc chrome, or barrier-type coatings, like epoxy and polyurethane. Moreover, another mitigating measure is the application of Corrosion Protection Sleeves (CPS). CPS, a corrugated polyethylene sleeve, is employed to shield steel rock bolts from corrosive environments (Nourizadeh et al. 2025b). As shown in Fig. 2, when properly encapsulated, CPS can significantly improve the durability of steel rock bolts in underground excavations (Villaescusa and Windsor 1999; Aziz et al. 2017). Therefore, the sleeved rock bolts (rock bolts covered by CPS) offer an innovative approach to overcoming the limitations of conventional reinforcement systems, particularly those related to corrosion vulnerability.

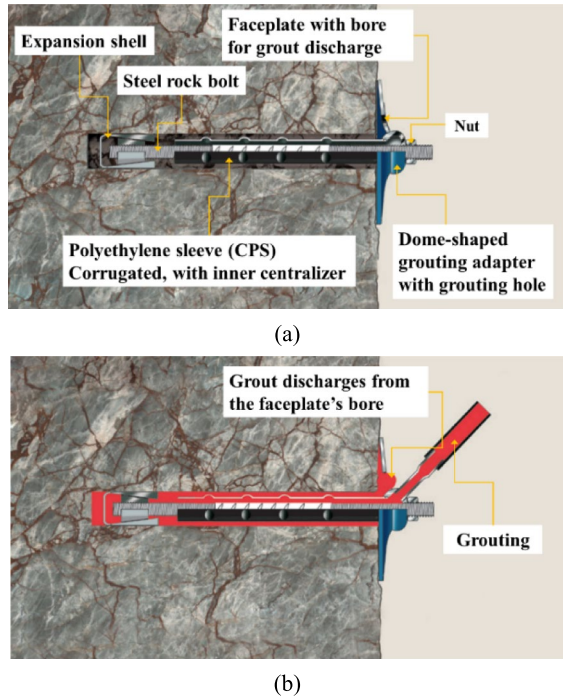

Fig. 2 A schematic view of the components of a sleeved rock bolting system: **a** pre-grouting and **b** post-grouting, adopted from (Dywidag; 2021)

1.3 Previous Studies

While rock bolts themselves are capable of withstanding significant axial and shear displacements, their corrosion protection systems, particularly CPS, may fail much earlier. Rock bolts and cable bolts generally offer large deformation capacity. However, when the goal is to preserve corrosion protection, the allowable deformation must be limited to the threshold at which the CPS remains intact (Bertuzzi 2004). It is noteworthy that damage to the CPS may expose rock bolts to corrosive conditions, undermining their effectiveness in ground control.

Despite the widespread application of CPS, there is a limited understanding of their mechanical integrity under axial and shear deformation. Based on the available literature, although an extensive number of studies have been conducted to assess the LTC of various rock bolt and cable bolt types, few experimental studies have been carried out to examine the performance of sleeved rock bolts.

As presented in Table 1, the first attempt to evaluate the behaviour of sleeved bolts was conducted by Villaescusa and Windsor (1999). In this study, a series of laboratory and field experiments was undertaken to evaluate the pull-out strength of sleeved bolts. Their laboratory tests focused on bolt rupture caused by relatively long encapsulation lengths (L_E). At the same time, the in-situ experiments examined the influence of host rock conditions, grouting, and ungrouting on bolt performance. Bertuzzi (2004) reported that the CPS sustained damage when subjected to approximately 15 mm of shear displacement. In another study, Aziz et al. (2017) carried out a laboratory investigation to assess the performance of sleeved cable bolts under shear loading conditions. Results from both single and double shear tests demonstrated that the CPS offered notable resistance to shear forces, remaining largely undamaged up to a maximum displacement of 33 mm.

Recently, Nourizadeh et al. (2025b) conducted a laboratory study to investigate the axial behaviour of sleeved rock bolts through three different pull-out testing setups. The results showed that the axial behavior and failure mechanisms of the sleeved bolts differ from conventional bolts. Two main failure modes were identified: bolt rupture and slip at the grout-CPS interface, influenced by L_E and test configuration. It was reported that due to poor adhesion and interlocking at the grout-CPS interface, shear stress did not reach its full potential, leading to grout damage and reduced bond strength. The CPS was found to remain intact up to 28 mm of axial displacement. It was also found that the maximum bond stress at the bolt-grout interface (6–8.7 MPa) was below the grout's shear strength, making failure at that interface unlikely.

1.4 Research Motivation and Objectives

Although previous studies have provided valuable insights into the behavior of sleeved bolts, further experimental research is needed to deepen our understanding of the axial and shear performance of grouted sleeved rock bolts. Notably, only one study has investigated the integrity of sleeved rock bolts under shear loading, leaving a gap in knowledge regarding their durability under double shear conditions.

Another issue is the interaction between CPS and the mechanical performance of rock bolts. While CPS effectively enhances corrosion protection, it also influences the pull-out characteristics and failure mechanisms, potentially altering the axial performance of sleeved rock bolts compared to conventional ones. Therefore, a comparative evaluation of

Table 1 Summary of the previous studies carried out on the performance of sleeved rock bolts

Ref	Bolt type	Test type	Host medium type	Displacement threshold (for having intact CPS)
Villaescusa and Windsor (1999)	Rock bolt	Pull-out	Steel pipe	–
Bertuzzi (2004)	Rock bolt	Single shear	Steel pipe & rock sample	15 mm
Aziz et al. (2017)	Cable bolt	Single & double shear	PVC pipe & concrete sample	33 mm
Nourizadeh et al. (2025b)	Rock bolt	Pull-out	Steel pipe	28 mm

the axial response of sleeved versus conventional rock bolts is necessary.

Furthermore, sleeved rock bolts are often encapsulated within steel pipes to simulate in-situ boundary conditions. However, this rigid confinement may overestimate the strength of the surrounding medium, affecting the load LTC (Mottahedi et al. 2025). Thus, assessing the influence of host medium type on axial performance is crucial to ensure a realistic simulation of field conditions. Ultimately, conducting a comparative analysis with earlier studies can provide important implications regarding the failure modes, load displacement thresholds, and the role of host medium in performance outcomes.

As shown in Fig. 3, the primary objective of this research is to evaluate the axial and shear behavior of sleeved rock bolts. In this regard, the study examines the influence of CPS on LTC by conducting pull-out tests on sleeved and conventional rock bolts encapsulated in different host mediums, an area that has not been sufficiently addressed in the literature. Additionally, through a series of laboratory experiments, the study investigates the displacement thresholds beyond which the integrity of the CPS deteriorates under shear loading. Meanwhile, comparing the single and double shear loading results can be helpful for evaluating the effect of host medium type on failure modes and shear behaviour profiles. To achieve these goals, a testing program has been developed, incorporating:

- Short encapsulation pull-out test (SEPT)
- Double embedment pull test (DEPT)
- Single shear test (SST)
- Double shear test (DST)

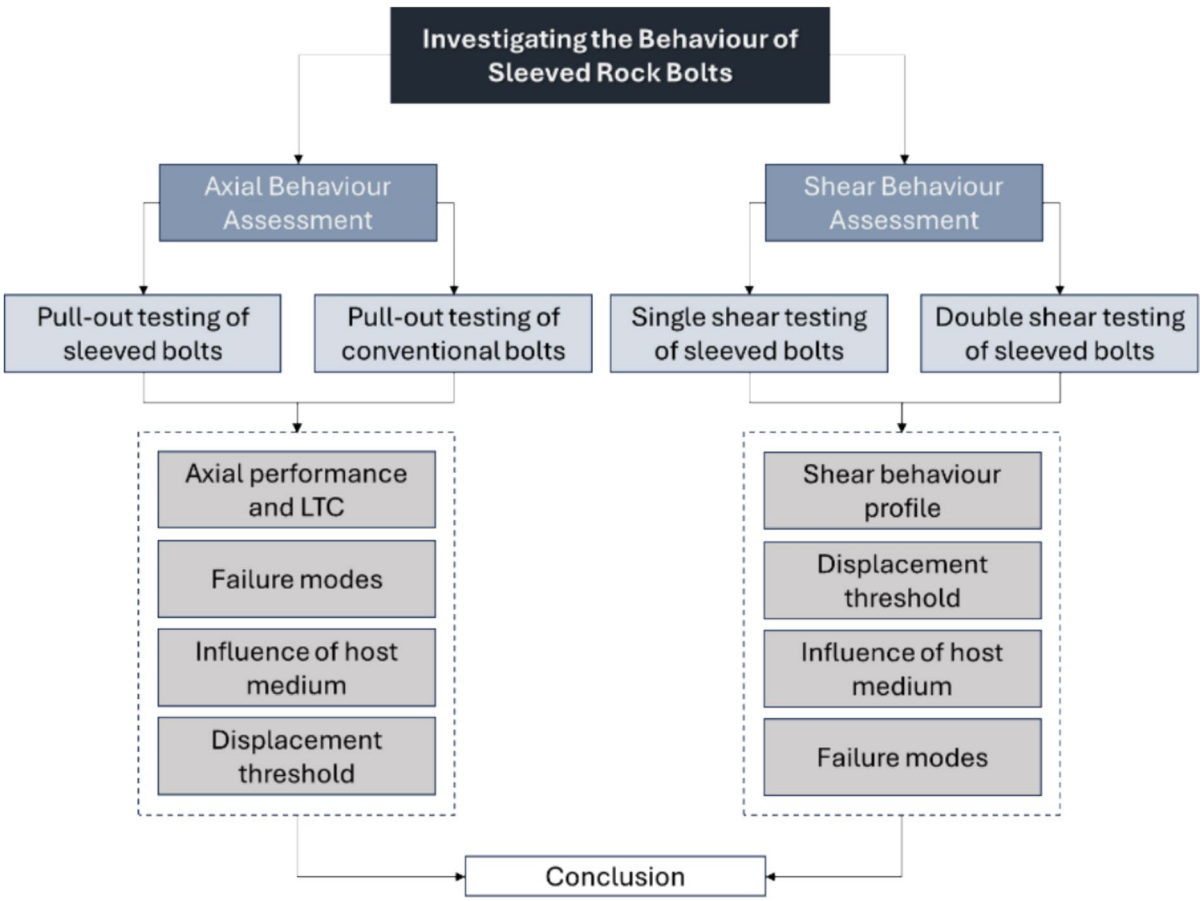

Fig. 3 The flow chart of the research objectives

The findings of this research can provide useful insights into the mechanical behavior and performance of sleeved rock bolting systems under various loading modes. These outcomes contribute to a more comprehensive understanding of their mechanical response and highlight potential vulnerabilities that may affect their long-term durability and reliability.

2 Research Design

2.1 Materials

(1) Rock Bolting System Components

As shown Fig. 4, the components of the rock bolt system include a steel rock bolt with a nominal diameter of 22 mm, featuring a domed-shaped grouting adapter at the bolt head to facilitate grout flow and anchorage. The rock bolt is protected by using a corrugated plastic sleeve (polyethylene), having an outer diameter of 30 mm and a wall thickness of 3 mm. The CPS shows two types of irregularities on its external

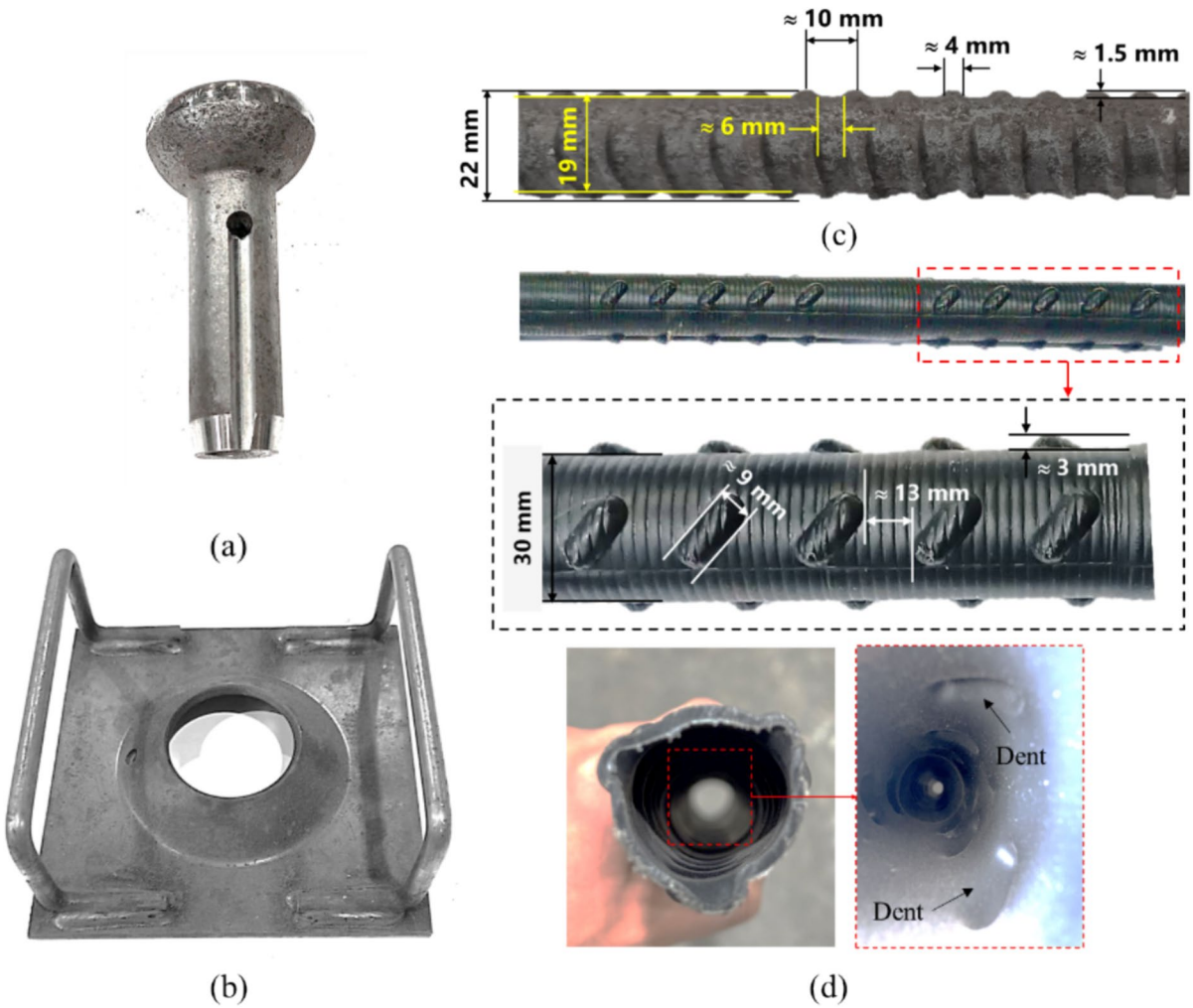

Fig. 4 The bolting system, including **a** spherical grout injection head, **b** dome plate, **c** rock bolt, and **d** CPS

surface, including circumferential threads and corrugations. Besides, the internal surface shows dents. A 5 mm thick steel dome plate with a central hole diameter of 50 mm is used to seat the domed-shaped bolt head. This plate serves as a load transfer interface and provides confinement at the collar of the borehole.

Figure 5 shows the tensile response of the rock bolts obtained through standardized tensile testing in accordance with British Standard BS 7861–1 (2007). The results of the three tests were consistent, and all bolts failed in tension, characterised by early necking along the strained length. The tensile failure surfaces of the snapped bolt sections were typically characterised by a cone and cup pattern. Based on the results, the average yield load was about 309 kN, while and Ultimate Tensile Load (UTL) reached 359 kN. Additionally, the maximum elongation before failure was approximately 33 mm. It indicates that, in the underground opening, the rock bolting system, reinforcing a block of rock mass, may fail under tension once the axial force exceeds the UTL (about 36 t) unless the failure occurs first at either the bolt-grout or rock-grout interfaces.

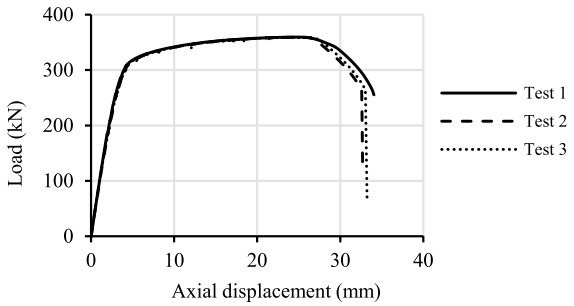

Fig. 5 The load–displacement curves of the tested rock bolts

(2) Grouting and Surrounding Materials

For grouting purposes, Crosbie (190) cement grout has been utilized in this study, prepared with a water-to-cement (w/c) ratio of 0.35 as was recommended by the rock bolt's supplier. To evaluate the compressive strength of the grout, 50 mm cubic specimens were cast and tested. As illustrated in Fig. 6a, the average 28-day Uniaxial Compressive Strength (UCS) was approximately 55 MPa.

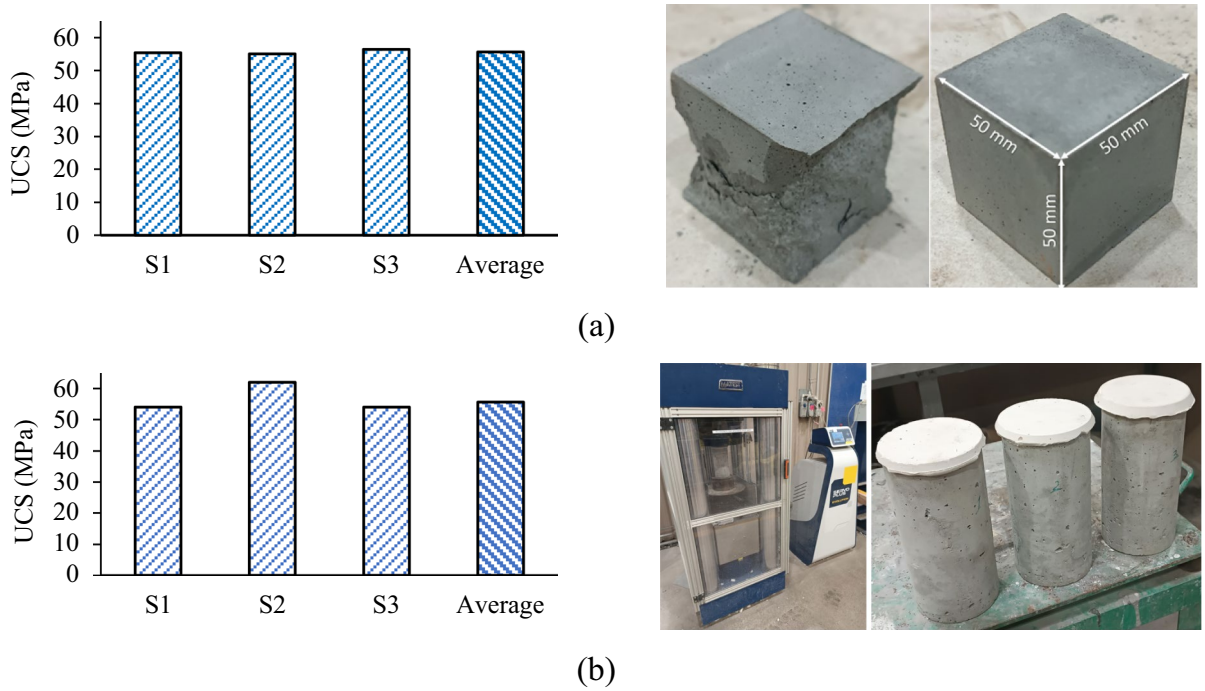

Fig. 6 The strength test results of the **a** grout and **b** concrete samples

Additionally, to simulate in-situ host rock conditions, the concrete medium used in this study has been prepared with gravel aggregate having a nominal maximum size of 5 mm. The mechanical properties of the concrete were evaluated by testing 100 mm diameter × 200 mm long cylindrical specimens (Fig. 6b). After 28-days of curing, the average UCS of the concrete was determined to be about 56 MPa.

2.2 Experimental Methods for Axial Behaviour Assessment

In this section, the proposed test configurations are designed to replicate practical field conditions where rock bolt failure is primarily governed by the slip mechanism. To simulate this failure mode, it is assumed that the mechanical expansion shell, normally responsible for providing a mechanical coupling through frictional contact with the borehole wall, has failed and no longer contributes to the system's structural integrity. This assumption isolates the load transfer mechanism to the encapsulated grout section, allowing for focused evaluation of slip-induced failure behavior. Besides, it is noteworthy that environmental factors, such as pH variation and humidity, which may influence the long-term performance of the bolting system, are not considered in this study. As demonstrated in Fig. 7, the axial behaviour of sleeved rock bolts has been investigated through three experimental campaigns within the pull-out testing program:

(1) Pull-Out Test on Conventional Rock Bolt

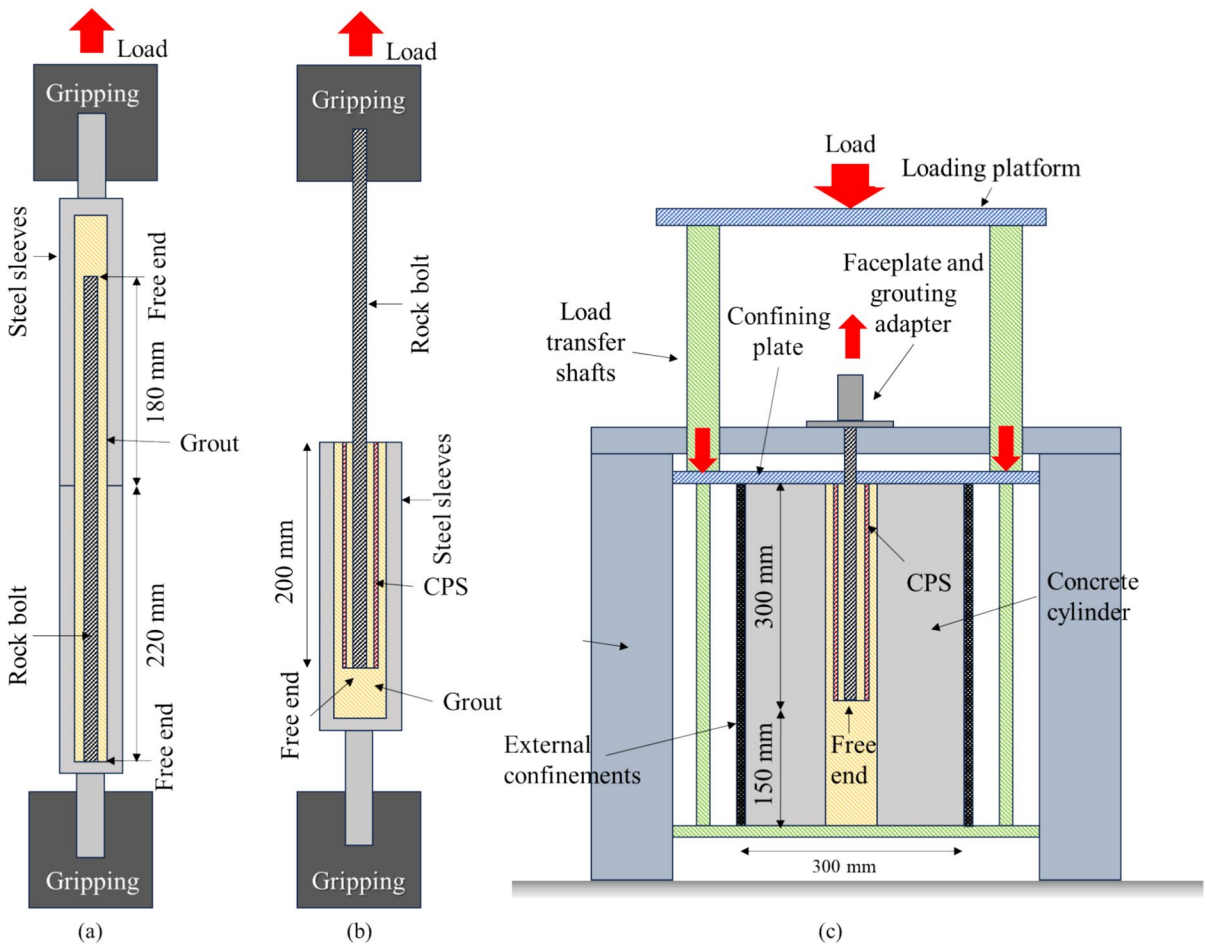

Fig. 7 Schematic view of the pull-out test designs

This test utilizes the DEPT method, employing different L_E with free ends, as shown in Fig. 7a. One side of the rock bolt is encapsulated to a greater length than the other. Thus, by applying axial load to the steel sleeve, only the shorter encapsulated side is mobilized, ensuring that the bolt would pull out from one end. This arrangement is designed to prevent bolt failure at higher applied loads due to the longer L_E. Therefore, bolt slip is the possible mode of failure in this configuration.

The steel split set system employed in this study is an enhancement to the procedures outlined in the British Standard BS 7861–2 (2009). In this DEPT system, two steel sleeves are bolted together to form a single central borehole with a 27 mm diameter and grooved internal walls, as shown in Fig. 8a. A 400 mm long section of rock bolt is installed and grouted within this borehole, resulting in an annular grout thickness of less than 5 mm.

Following a 28-day curing period, the test specimen was mounted in the grips of the 50 t Instron universal testing machine. The system was configured for axial tensile loading, with both load and displacement continuously monitored and recorded using the machine's data logging unit. Additionally, all pull-out tests were conducted under displacement-controlled conditions at a constant rate of 3 mm/min, ensuring consistent loading across specimens.

(2) Pull-Out Test on Sleeved Rock Bolt

This test configuration follows the SEPT method, using a sleeved rock bolt with a L_E of 200 mm and a free end, as shown in Fig. 7b. In this test setup, the axial load is applied directly to the rock bolt, replicating in-situ pull-out conditions where the load transfer occurs through the bolt itself. The L_E of 200 mm is selected to prevent tensile failure of the rock bolt under higher axial loads, isolating the failure mechanisms to the bond interfaces. As a result, the test is designed to evaluate potential failure at either the bolt-grout interface or the grout-CPS interface, providing insight into the influence of the CPS on load transfer characteristics and overall axial performance.

As shown in Fig. 8b, the steel confinement in this SEPT configuration consists of two primary components: an internal sleeve and an external sleeve. When these components are aligned and securely bolted together, they form a central grooved borehole with a diameter of 42 mm, designed to simulate the encapsulation environment for sleeved rock bolts. To prepare the test specimen, a 200 mm long section of the CPS is first grouted into the central borehole using the grout. Next, the rock bolt is installed to a depth of 200 mm within the grouted sleeve, using the same grout material to ensure uniform bonding conditions.

Following a 28-day curing period, the specimen is mounted in the grips of the 50 t Instron machine. The bolt is subjected to axial tensile loading at a displacement-controlled rate of 3 mm/min, and the test continues until debonding occurs at one of the interfaces. Load and displacement data are continuously recorded using the data logger unit.

(3) Pull-Out Test on Sleeved and Conventional Rock Bolt in Concrete Medium

As shown in Fig. 7c, in this test configuration, the rock bolt is pulled out of the host medium, externally confined by using two 30 mm-thick half-cylinder steel clamps, based on a push-to-pull loading mechanism. In this regard, once the axial load is applied to the loading platform, it is conveyed to the vertical confining plate by the load transferring shafts, and then the host medium is pushed down as part of the moving elements (Anzanpour 2022). Therefore, based on the described loading mechanism, this test setup is called the Reverse Pull-out Test Machine (RPTM). In this configuration, the bolt tensile failure and debonding at one of the interfaces are possible failure modes.

In this design, 300 mm diameter concrete cylinders are employed as the host medium to evaluate the influence of the surrounding material on axial performance. Chen et al. (2017) reported that the LTC of the bolt during pull-out testing increased with the diameter of the host medium up to 300 mm, beyond which the LTC was approximately stable. Based on this finding, a host medium diameter of 300 mm was selected in this study. In addition, the previous laboratory pull-out tests on rock bolts demonstrated that an L_E of 320 mm resulted in higher pull-out capacities compared to a L_E of 300 mm, with the load approaching the bolt's yield strength (Aziz et al. 2016). Therefore, a 300 mm L_E has been selected for the current test configuration to maintain the applied

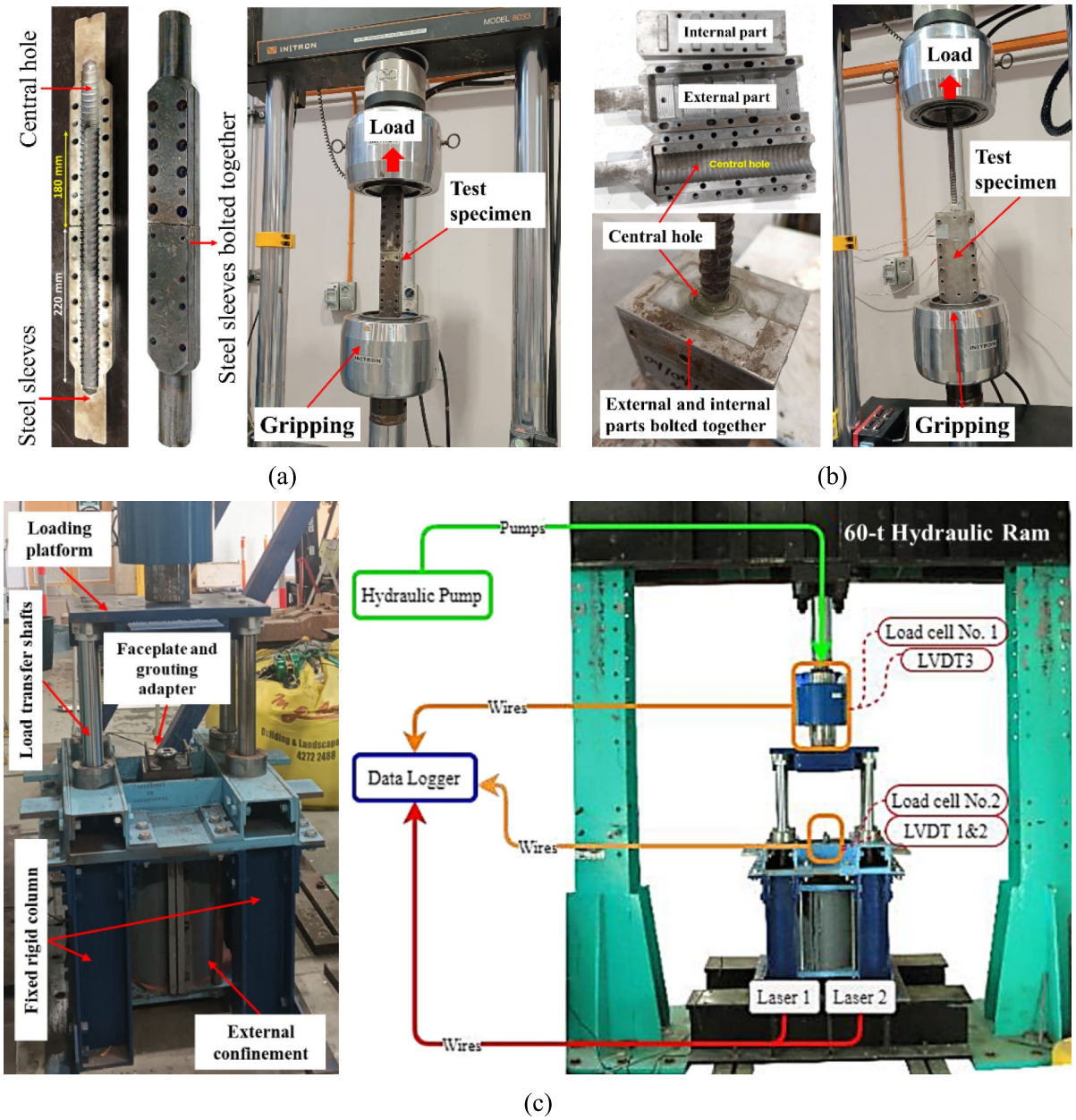

Fig. 8 The test arrangements: **a** pull-out test on conventional rock bolt, **b** pull-out test on sleeved rock bolt, and **c** pull-out test on sleeved and conventional rock bolt in concrete medium

load within a controlled range near the yield threshold and to prevent the risk of bolt tensile failure.

As illustrated in Fig. 7c, the sleeved rock bolt with an effective L_E of 300 mm and a free end is installed in the 42 mm rifled borehole. Then, the conventional rock bolt without a CPS is installed and tested under the same conditions. It allows for an evaluation of the axial performance differences between sleeved and conventional rock bolts when subjected to the same L_E and loading configurations. This setup enables direct assessment of the host medium's effect on LTC, overall bond behavior, and failure mode.

For pull-out testing, following a 28-day curing period, the RPTM is mounted beneath the 60-t

hydraulic ram. In all tests, the displacement rate of 3 mm/min is set. Throughout the test, axial loads and vertical displacements are continuously monitored and recorded using a data acquisition system (Fig. 8c).

2.3 Experimental Methods for Shear Behaviour Assessment

To evaluate the shear behavior of sleeved rock bolts, both SST and DST configurations have been employed, as schematically illustrated in Fig. 9. In the SST method, the rock bolt is sheared through one shear plane while the DST approach involves shear testing at two points on the rock bolt (Aziz et al. 2003). These configurations are designed to simulate shear loading conditions representative of in-situ rock bolt applications. The host medium surrounding the sleeved rock bolt varied between the two configurations to investigate its influence on shear response and failure mechanisms. In both SST and DST set-ups, shear loading is applied until a pre-determined vertical displacement is reached. This displacement threshold is selected to enable assessment of the CPS integrity under shear deformation.

(1) SST on Sleeved Rock Bolt

The small-scale guillotine-type SST is conducted in accordance with the British Standard BS 7861–2 (2009) to evaluate the shear response of sleeved rock bolts. In this configuration, the host medium consisted of a smooth-walled PVC pipe, providing a controlled and uniform boundary condition for consistent shear loading. As illustrated in Fig. 9a, the sleeved rock bolt is encapsulated within the PVC tube, and a 12 mm wide ring strip is removed from the mid-section to expose the CPS. This modification enabled direct visual inspection of the CPS during and after shear loading.

Based on findings by Aziz et al. (2017), a shear displacement of 40 mm was identified as a critical threshold for CPS damage. Accordingly, this displacement has been used as the maximum deformation in the initial test. If damage was observed, subsequent tests were conducted with systematically reduced shear displacements to determine the onset of CPS failure. In this regard, following a 28-day curing period, the SST specimen is mounted on the 50-t Instron machine Fig. 10a. All tests are conducted at a constant rate of 3 mm/min. Besides,

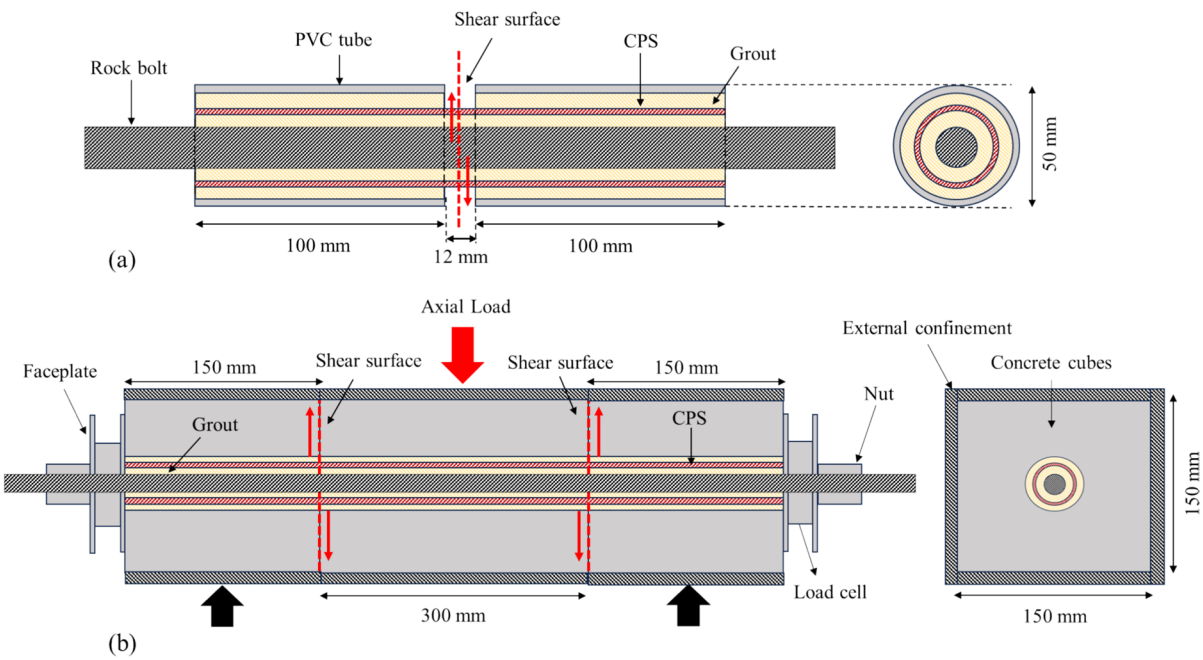

Fig. 9 Schematic view of the shear tests design

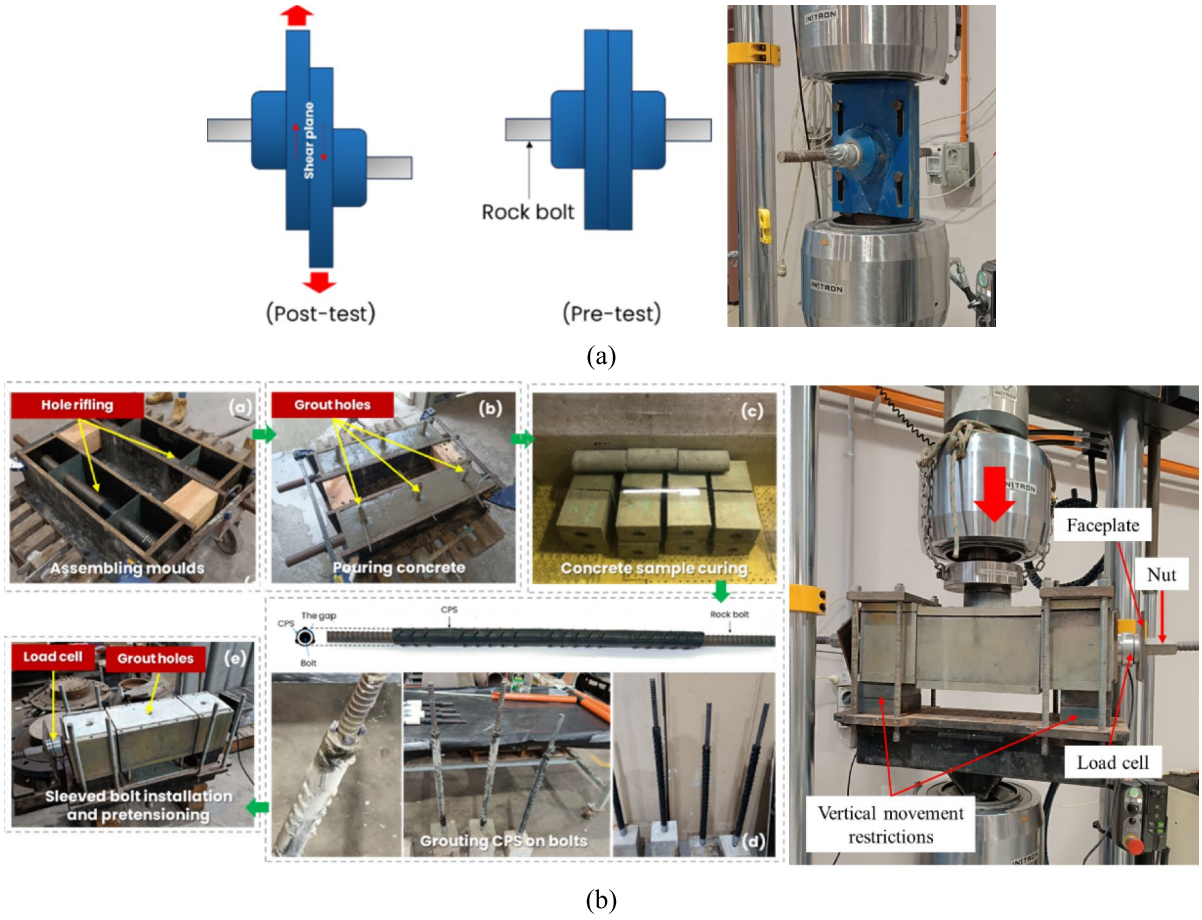

Fig. 10 The test arrangements: **a** SST on sleeved rock bolt and **b** DST on sleeved rock bolt

after each test, the specimen is dismantled and inspected for signs of CPS damage.

Table 2 The Summary of the conducted pull-out tests on conventional and sleeved rock bolts

#	Host medium type	Bolt condition	P_{max} (kN)	$\delta_{P_{max}}$ (mm)	K (kN/mm)	Ave. P_{max} (kN)	Ave. K (kN/mm)	Ave. $\delta_{P_{max}}$ (mm)	Unit load per $L_E{}^*$ (kN/mm)
1	Steel	Conventional	128.4	1.9	96.9	132.5	110.7	1.8	0.74
2		Conventional	136.5	1.7	124.4				
3		Sleeved	111.5	7.5	55.9	101.9	56.9	9.8	0.51
4		Sleeved	102.6	13.5	66.4				
5		Sleeved	94.2	7.4	50.0				
6		Sleeved	99.2	10.6	56.9				
7	Concrete	Conventional	205.6	10.3	22.8	–	–	–	0.68
8		Sleeved	117.8	16.3	10.4	–	–	–	0.39

*P_{max}/L_E

(2) DST on Sleeved Rock Bolt

As shown in Fig. 9b, the DST configuration utilizes concrete cubes as the host medium to simulate field conditions. The cube dimensions are sufficient for the test type, given the use of small-diameter rock bolts and the requirement for limited vertical displacement (Aziz et al. 2003). To replicate external confinement, each concrete cube is enclosed with 20 mm-thick steel plates. The DST assembly process involves grouting the CPS onto the rock bolt, casting concrete blocks with 42 mm rifled central boreholes, and encapsulating the sleeved rock bolts into the boreholes (Fig. 10b). Next, the bolts are pretensioned to 50 kN, and axial forces are monitored using 75-t capacity hollow load cells positioned on either side of the specimen.

Similar to the SST configuration, a maximum vertical displacement of 40 mm is applied in the initial test, based on CPS damage thresholds reported by Aziz et al. (2017). If damage is observed, subsequent tests are conducted with systematically reduced shear displacements to identify the onset of CPS failure. Each test is performed on a new DST assembly under displacement-controlled loading at 3 mm/min. Besides, after each test, the DST specimen is dismantled, and the CPS is visually inspected for damage.

3 Results and Discussion

3.1 Axial Behaviour Assessment and Comparative Analysis

(1) Load Transfer Capacity

At this stage, a total of eight pull-out tests were conducted. The results are summarized in Table 2 and the load–displacement curves are illustrated in Fig. 11. Based on the outcomes, regardless of whether the pull-out tests were conducted in steel or concrete medium, the load–displacement curves can be divided into four regions, including elastic (initial linear), transition, bond failure, and residual load regions, as shown in Fig. 12.

In the early stage of loading, the curves show a linear relationship, indicating elastic behavior with no observable debonding, where the load is transferred through the grout medium. The slope of this region represents the pull-out stiffness (K). In the transition region, the curve begins to bend, suggesting the onset of micro-cracking or bond degradation at one of the interfaces. Once the peak pull-out load (P_{max}) is reached, the third region starts, followed by a drop in load, indicating bond failure. This is the point at which the LTC decreases, and the bolt begins to pull out. Finally, in the residual region, the load stabilizes at a lower level, reflecting the residual capacity of the bolting system to carry load despite damage. At this stage, the bond relies solely on residual frictional resistance, and further displacement occurs with minimal increase in load.

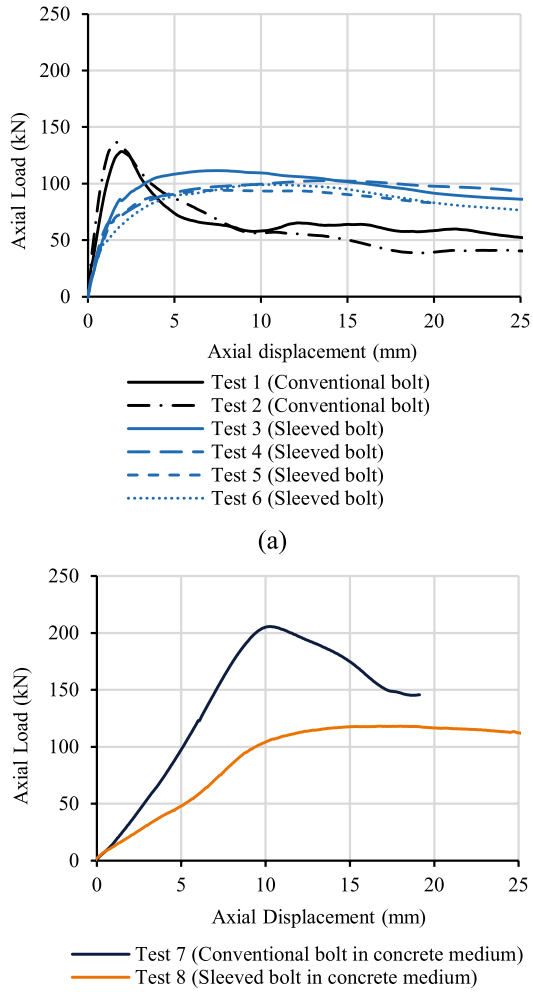

Fig. 11 The load–displacement curves of the pull tested specimens in **a** steel medium and **b** concrete medium

A comparative analysis of the load–displacement curves reveals that conventional rock bolts show a higher average pull-out stiffness (110.7 kN/mm) in the initial linear region than sleeved rock bolts (56.9 kN/mm). Similar behaviour was also observed when concrete cylinders were used as the host medium (see Fig. 11b). These results indicate that, regardless of the host medium type, the conventional bolts offer greater resistance to axial displacement and demonstrate enhanced initial anchorage and LTC. The reduced stiffness in sleeved bolts may be attributed to the presence of the CPS, which introduces a more yielding interface between the bolt and grout.

Figure 11 also shows that sleeved bolts demonstrated lower peak loads but allowed for greater axial displacement ($\delta_{P_{max}}$) prior to debonding, indicating a more ductile response. The presence of the CPS likely alters the bonding mechanics, distributing stress more evenly, resulting in a broader transition region. The extended transition region could imply a more gradual failure and a safe allowance of more roof convergence, allowing for early warning and intervention before the instability stage is reached.

The post-peak behaviors also lead to further comparisons. In this regard, the conventional bolts show a sudden reduction in LTC following debonding, whereas sleeved bolts show a more gradual decline, suggesting that the CPS contributes to sustained load transfer through mechanical interlocking or residual friction. This is supported by the higher residual load levels observed in the sleeved bolts, indicating more effective post-failure performance. Despite the enhanced post-failure performance of sleeved rock bolts, conventional bolts demonstrated higher load efficiency per unit L_E across both steel and concrete medium, as presented in Table 2. This is likely due to the lack of adhesion and interlocking at the grout-CPS interface in sleeved bolts, which reduces the effectiveness of load transfer along the encapsulated length. Therefore, while sleeved bolts offer more ductile response, conventional bolts may be more effective in ground conditions where higher pull-out stiffness and load efficiency are needed.

Additionally, lower unit load values per L_E were observed in pull-out tests conducted within concrete medium compared to steel. This discrepancy can be attributed to the inherent stiffness differences between the host mediums. Steel sleeves provide

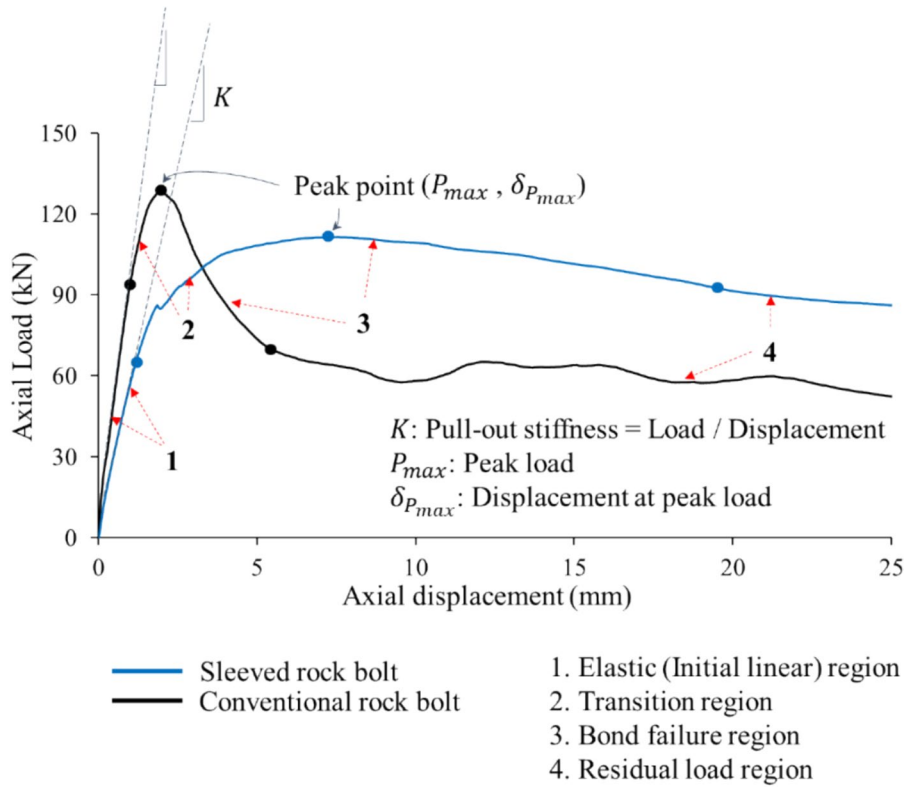

Fig. 12 A comparison between the various regions of the load–displacement curves of the tested rock bolts

a stiffer confinement, enhancing the bond strength and load transfer efficiency, whereas concrete, being less stiff, results in reduced confinement. This variation in the host medium also affects the pull-out stiffness of both sleeved and conventional bolts during the initial loading phase. As shown in Fig. 11 and Table 2, the pull-out stiffness values observed in concrete medium are considerably lower than those obtained in steel medium. These findings highlight the influence of host medium stiffness on pull-out performance.

(2) Failure Mechanism

In the case of sleeved rock bolts, since the contribution of the expansion shell was excluded from this study and the bolt was permitted to slip at its free end, the main failure mechanism occurred at the interface between the grout and CPS. This failure mode was revealed in the post-test observations, as illustrated in Fig. 13a, b. In both concrete and steel medium, the axial loading led to the extraction of the grout and bolt column from the specimen, indicating a loss of bond integrity.

Typically, for short L_E, debonding occurs at the bolt-grout interface. However, in this study, debonding occurred at the grout-CPS interface, which may be due to the lack of sufficient interlocking and adhesion at the grout-CPS interface. This resulted in the sleeved bolts showing lower pull-out capacities compared to the conventional bolts. The lack of interlocking allowed the induced tensile stress to exceed the bond strength at the grout-CPS interface. Furthermore, the low frictional resistance between the grout and the inner surface of the CPS may be due to the specific configuration of the inner surface of the CPS. It is worth noting that similar failure behaviour was

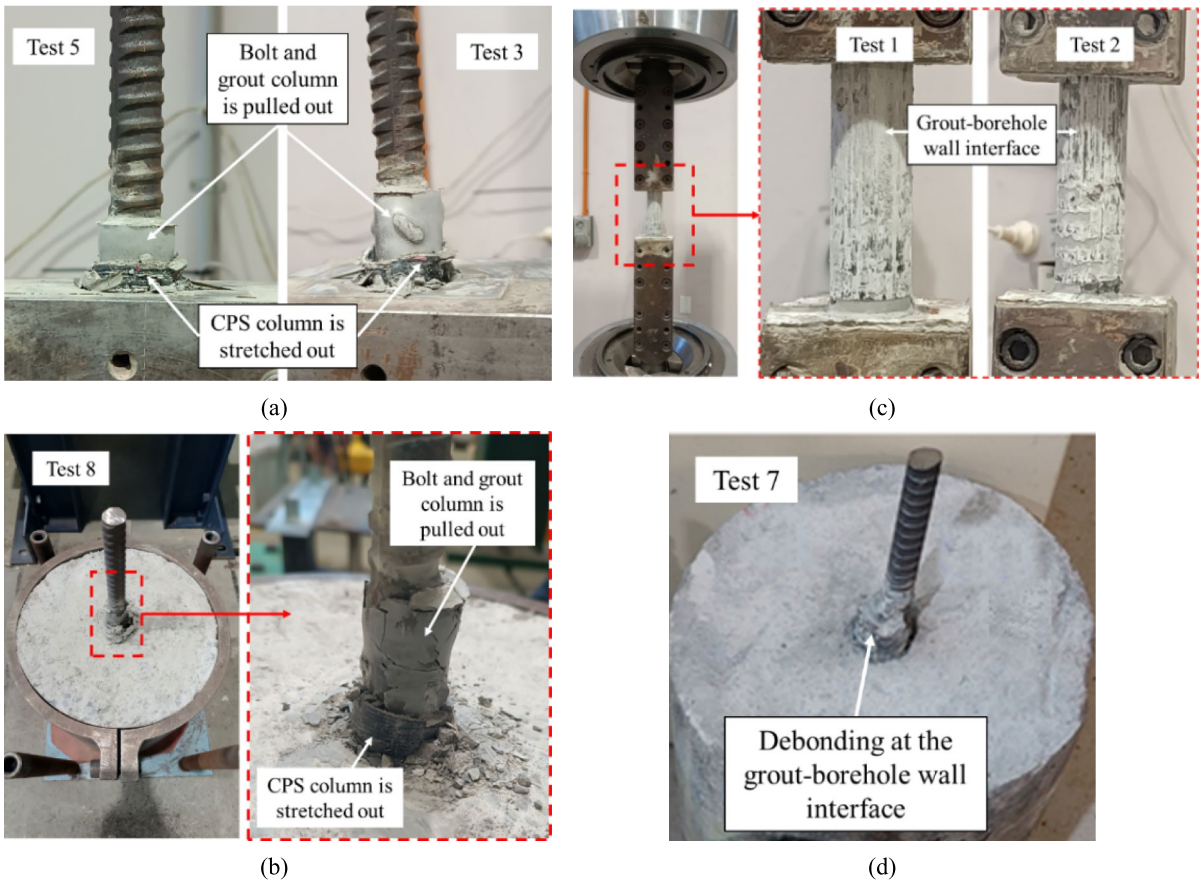

Fig. 13 The failure mechanisms of the sleeved and conventional rock bolts

reported by Nourizadeh et al. (2025b), where bolt slippage was also allowed in the test arrangement.

For the conventional rock bolts, the test results indicate that the bond strength between the rock bolt and the grout column was greater than that between the grout and the borehole wall. As illustrated in Fig. 13c, d, this led to debonding occurring at the grout-borehole wall interface. This behavior suggests that the bolt's surface profile, mainly the rib height and spacing, provided an enhanced mechanical interlocking, improving the bond strength at the bolt-grout interface.

Furthermore, the structural integrity of the CPS under axial loading was evaluated. As shown in Fig. 14, the CPS experienced partial pull-out and stretching during the loading process, which in some cases led to severe sleeve rupture and surface cracking. It was found that the extent of CPS damage increased with axial displacement. In Test 3 and 8, where axial displacement was higher, severe damages were observed, including complete rupture and extensive cracking of the CPS (see Fig. 14a, e). This raises concerns regarding the long-term integrity of the sleeve, especially in terms of potential cracking, water ingress, and subsequent corrosion of the rock bolt.

By reducing the axial displacement, it was found that the severity of damage was reduced. At a vertical deformation of 25 mm, a few of the CPS's ribs were damaged without any longitudinal cracking on the CPS surface (see Fig. 14b, d). Meanwhile, when the displacement was reduced to 20 mm, localized damage to the ribs was formed, but no significant cracking was noted (see Fig. 14c). Based on the results, to find the axial displacement threshold below which this specific type of CPS remains undamaged and intact, further investigations are needed.

3.2 Shear Behaviour Assessment and Comparative Analysis

(1) Shear Behaviour Profile

The summary of the conducted SSTs and DSTs, including the peak shear loads (S_{max}), shear displacements (δ_S), and the obtained load–displacement curves are shown in Table 3 and Fig. 15, respectively. Based on the results, the shear process of the tested sleeved bolts can be divided mainly into three regions, including high stiffness (k_H, elastic), low stiffness (k_L, plastic), and failure regions as illustrated in Fig. 16.

As illustrated in Fig. 16, the initial region is characterised by a linear relationship between the shear load and displacement, indicating elastic deformation of the bolt-grout-host medium system. The stiffness in this region is governed by factors like the bolt's modulus of elasticity and concrete strength (Li et al. 2016; Gregor et al. 2024a). As shown in Table 3, the DST samples showed higher average initial stiffness (23.9 kN/mm) than the SST samples (10.7 kN/mm), indicating more effective confinement and load transfer in the DST. The high stiffness region terminates at the elastic yield point (the turning point), where microcracking initiates in the grout and concrete medium, but the bolt remains undeformed. Following the turning point, there is a none-linear transition zone, and the plastic stage starts.

Plastic stage is characterised by the sample yielding and debonding from the grout (Grasselli 2005; Jalalifar and Aziz 2010). In the DSTs, this transition is relatively abrupt, indicating a clear onset of plastic deformation and debonding at the grout-CPS interface. In contrast, the SSTs show a smoother transition, showing a gradual redistribution of stresses and progressive yielding. This stage is marked by the formation of plastic hinges in the sleeved bolt near the shear plane, crushing of the concrete medium in the compression zones (where the sleeved bolt starts to deflect), and progressive debonding between the sleeved bolt and grout (Jalalifar and Aziz 2010; Gregor et al. 2024b). The reduced slope reflects a drop in shear stiffness, with the bolt accommodating larger displacements under slowly increasing load. At the higher displacements, the sleeved bolt reaches its ultimate capacity. This is followed by a rapid decline in the LTC, indicating structural failure.

(2) Shear Displacement Threshold

The outcomes of the carried out shear tests indicate the influence of vertical shear displacement on the CPS integrity. In the DST, as shown in Fig. 17, as the vertical displacement increases from 20 to

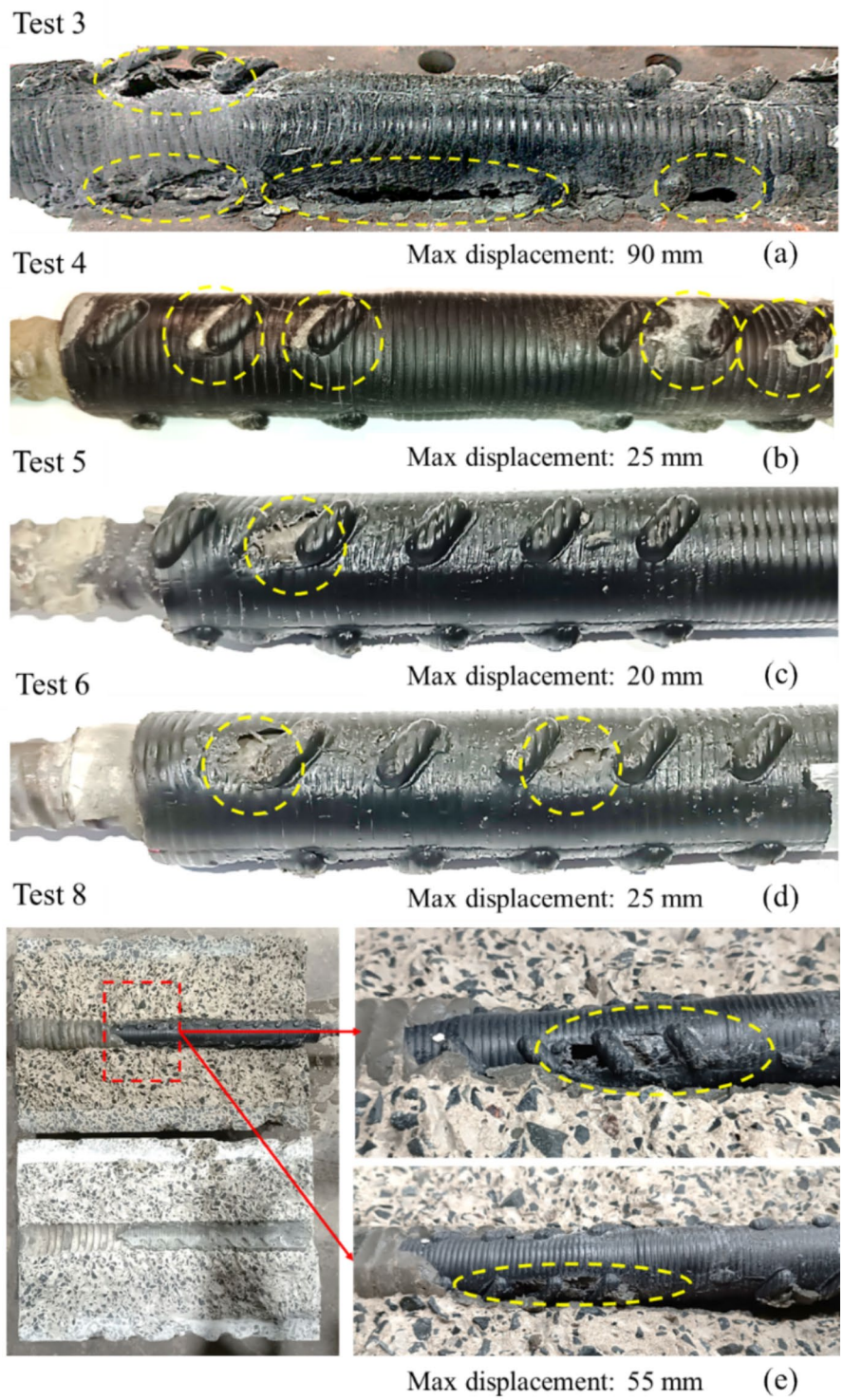

Fig. 14 The post-test conditions of the CPS

Table 3 Summary of the conducted single and double shear tests on sleeved rock bolts

#	Test type	δ_S (mm)	S_{max} (kN)	k_H (kN/mm)		k_L (kN/mm)	
				Value	Ave	Value	Ave
1	DST	40	282.2	22.8	23.9	6.1	5.5
2		30	196.7	27.4		4.7	
3		25	201.6	21.3		5.3	
4		20	192.3	24.1		5.8	
5	SST	40	240.1	10.8	10.7	5.5	5.2
6		30	183.3	10.5		5.4	
7		25	173.2	12.3		5.9	
8		20	115.4	9.2		4.0	

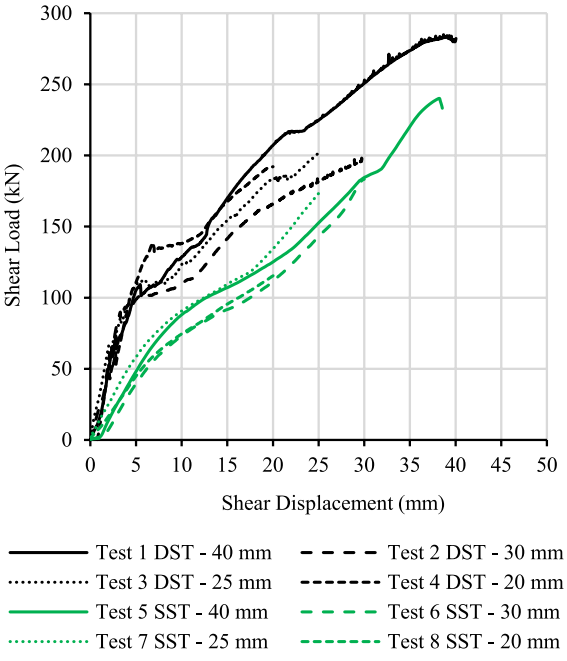

Fig. 15 The shear load–displacement curves of the sleeved rock bolt

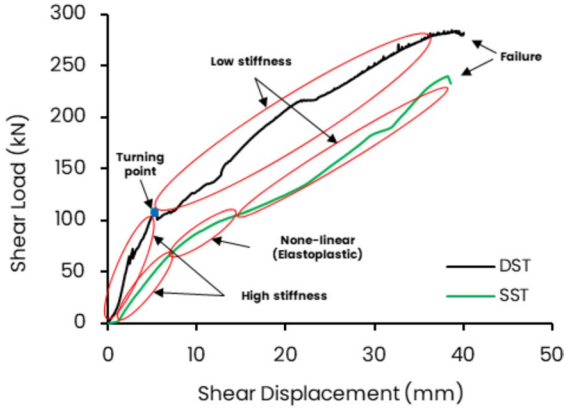

Fig. 16 A comparison between the various regions of the shear load–displacement curves resulted from DST and SST

40 mm, the severity of damage transitions from superficial bruising to full structural cracking.

It can be seen that the sleeved bolts subjected to up to 20 mm of shear displacement did not show any visible cracking, indicating that the material remained within its elastic or early plastic range. In this case, the CPS only showed slight surface bruising. Figure 18a shows that there is no noticeable bolt's plastic deformation at 20 mm displacement. At 25 mm displacement, more bruising was observed. Although no cracks were visible, this stage likely marks the onset of micro-structural degradation, which may not be externally detectable but could compromise long-term performance (e.g., water ingress, corrosion initiation). In addition, as shown in Fig. 18b, the bolt started to plastically deform at 25 mm displacement, characterised by forming the plastic hinge points.

At 30 mm displacement, the CPS showed more damage, characterized by noticeable surface deformation and material fatigue. While still not cracked, it seemed that the CPS is approaching its critical strain limit, and any additional displacement could trigger rupture. At this level of displacement, the bolt showed more plastic deformation (Fig. 18c). Ultimately, at 40 mm displacement, visible rupture occurred, indicating that the CPS has exceeded its tensile strain capacity. This rupture marks the structural failure threshold, beyond which the CPS can no longer maintain its mechanical integrity or provide effective environmental sealing against water ingress or corrosion.

As illustrated in Fig. 18d, the deformation of the bolt extended with increasing shear displacement. The grout likely experienced cracking and debonding, particularly near the plastic hinges. Although the bolt seems to be able to accommodate more shear displacement, the loss of CPS integrity can adversely affect its long-term durability. It is also noteworthy that the damage patterns on the left and right shear surfaces are largely symmetrical across displacement levels, showing that the shear loading was evenly distributed. This symmetry implies that the observed damage is primarily a function of vertical displacement level rather than asymmetric loading or material inconsistencies.

In the SST, the increase in shear displacement was correlated with the severity of the CPS damage. The damage intensified with increasing vertical displacement, ultimately leading to sleeve cracking between 40 and 25 mm of displacement.

As shown in Fig. 19, at 20 mm displacement, the CPS was stretched but remained intact, and it seemed that the material was still in an elastic or early plastic stage. It can also be seen from Fig. 20 that the bolt remained at its elastic region after 20 mm displacement. At 25 mm displacement, the CPS showed bruising, indicating surface deformation. It is likely that some minor but invisible cracks may have formed within the sleeve. At 30 mm displacement, cracking was evident, showing that the CPS can no longer function effectively. Finally, the CPS was fully snapped at 40 mm displacement. At this stage, the CPS lost its ability to provide confinement or protection to the bolt, and the system is no longer functional. Detailed inspection of the tested specimens revealed that the onset of visible CPS cracking consistently initiated at approximately 25 mm of shear displacement.

Based on the results of both SST and DST, 25 mm appears to be the upper safe limit for vertical shear displacement before irreversible damage initiates. Beyond this point, the risk of cracking and long-term degradation increases considerably. It is noteworthy that Bertuzzi (2004) reported that 15 mm is the safe limit for the shear displacement of sleeved bolts. The variations may be attributed to the types of CPS and rock bolt and the strength of the host medium employed in the experiments. Additionally, the outcomes of this research show that the CPS material may lack sufficient ductility or toughness to accommodate large shear displacements. Thus, future designs could benefit from measures like enhanced rib geometry to distribute stress more evenly and thicker wall sections to delay damage initiation.

(3) Host Medium Influence

The results of shear tests indicate that the host medium influences both LTC and the failure mode of the samples. The LTC observed in the shear load–displacement curves (see Fig. 15) varies between the DST and SST, primarily due to differences in the host medium strength and its stiffness. In the SST, the sleeved bolt was encapsulated within a rigid PVC tube, which provides minimal deformation and restricts stress redistribution. On the other side, the DST is conducted within a concrete medium, which is deformable and susceptible to localized crushing under shear loading. During the shear movement, crushing of the host medium and encapsulation medium occurs due to localised stresses, and load transfer occurs by the rock bolt bending (deflection) at the plastic hinge points (see Fig. 21) (Galvin 2016; Chen et al. 2025).

The deflection of the bolt converts part of the applied shear load into axial load along the bolt length. This axial engagement increases the overall resistance of the bolt to shear failure. Therefore, in DST, a higher shear load is needed to reach ultimate failure compared to SST.

This mechanism is evident when comparing shear tests conducted in host mediums with different strengths. For instance, in granite with a UCS > 130 MPa, the host medium remains largely intact, and the bolt fails primarily in shear. On the other hand, in weaker materials like mudstone (UCS ≈ 40 MPa), the host medium undergoes more crushing, resulting in greater bolt bending and axial tension. This results in a combined tensile-shear failure mode, where the bolt is subjected to higher loads due to the additional axial stress component induced by host medium deformation. This behavior was also observed in the present study.

As shown in Fig. 22a, at 40 mm of displacement, the sleeved bolt experienced shear failure, characterized by a clean separation across the shear plane. This indicates that the bolt was subjected to a pure shear loading condition, with minimal axial stretching or bending. In contrast, Fig. 22b illustrates that

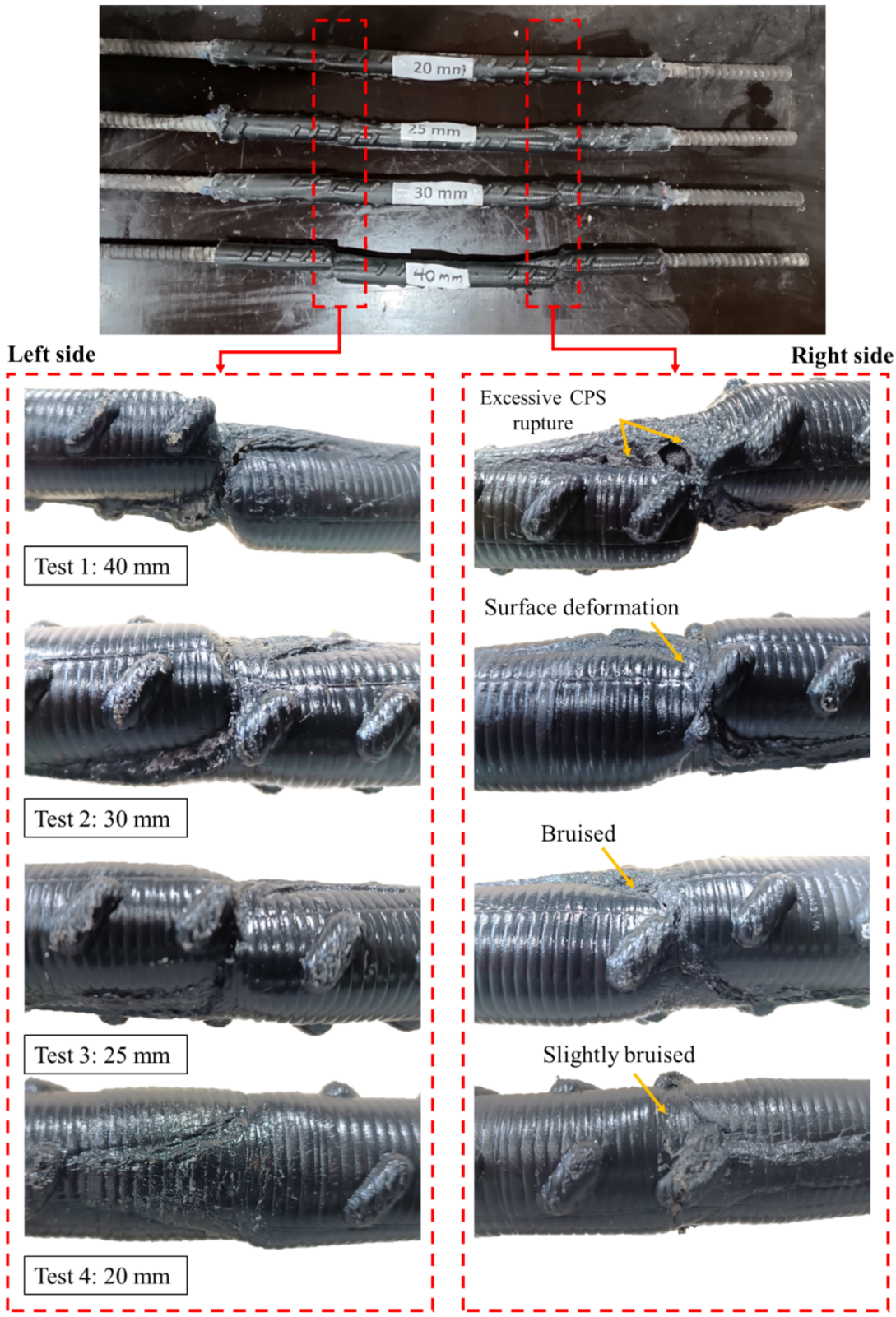
20 mm
25 mm
30 mm
40 mm
Left side
Right side
Excessive CPS rupture
Test 1: 40 mm
Surface deformation
Test 2: 30 mm
Bruised
Test 3: 25 mm
Slightly bruised
Test 4: 20 mm

◂**Fig. 17** Detailed post-test views of the double sheared sleeved bolts

the bolt experienced a combined tensile-shear deformation mode. The tensile-shear mechanism occurs when shear loads are redistributed into axial tension along the bolt length, facilitated by the deformation of the concrete and the bolt deflection. In heterogeneous rock masses, such as those with alternating zones of high and low strength, the bolt is more likely to experience a tensile-shear failure mode. This mode is more representative of in-situ conditions, where localized rock crushing, bolt bending, and grout debonding collectively contribute to the failure process. Therefore, it is essential to predict the possible failure mechanisms based on rock mass quality.

4 Future Research Directions

This research evaluated the performance of sleeved rock bolts under both axial and shear loading conditions. While the results offer useful insights, the limited number of test scenarios constrains the statistical robustness and repeatability of the findings. A broader range of test configurations is necessary to mitigate the influence of experimental variability and reduce the risk of biased conclusions. For instance, the influence of the expansion shell on the axial behaviour of the bolt was ignored in the present paper, which needs to be studied in the future.

Based on the current findings and identified limitations, several directions are proposed for future research. First, additional pull-out and shear tests are required to draw more definitive conclusions regarding the structural integrity and LTC of the sleeved bolt. Second, a detailed microscopic examination of fracture surfaces on the sleeves should be conducted to better understand failure mechanisms at the material level. Third, the influence of grout strength on the mechanical performance of sleeved bolts demands further investigation, particularly through systematic variation of w/s ratios and curing durations.

5 Conclusions

This research provided an experimental investigation on the sleeved rock bolts, focusing on their axial and shear performance to address the gaps in the existing literature. The findings offer useful insights into the mechanical behavior of these ground reinforcement systems, highlighting both their advantages and potential limitations under various loading conditions.

The axial pull-out tests revealed that the presence of a CPS alters the load transfer characteristics and failure mechanisms of the rock bolt system. This finding is of practical importance as it demonstrates that the sleeved bolts, unlike the conventional bolts, show a more ductile response. It may provide a safety mechanism in geotechnical applications by allowing for greater axial deformation before debonding. This yielding behavior can serve as an early warning of potential ground instability, enabling practical intervention and mitigating the risk of catastrophic failure. Furthermore, the sustained load transfer after debonding, characterized by higher residual loads, shows their load-bearing capacity after the failure.

Similarly, the shear tests offer useful indications for field engineers. The identification of a consistent shear displacement threshold (approximately 25 mm) beyond which the integrity of the CPS is compromised is a useful finding for design and maintenance protocols in underground excavations. It was found that while the rock bolt itself may accommodate larger displacements, the loss of the CPS means the system is no longer providing its intended long-term corrosion resistance. This research presented a boundary condition for when a sleeved bolt system may be considered functionally compromised, guiding inspection routines and replacement strategies. The comparative analysis also reinforces the importance of the bolt's interaction with the host medium, highlighting how the deformability of the surrounding rock or concrete can influence the LTC and failure mode.

Overall, while sleeved rock bolts offer enhanced long-term corrosion resistance and a ductile response, their mechanical performance is influenced by both the presence of the CPS and the stiffness of

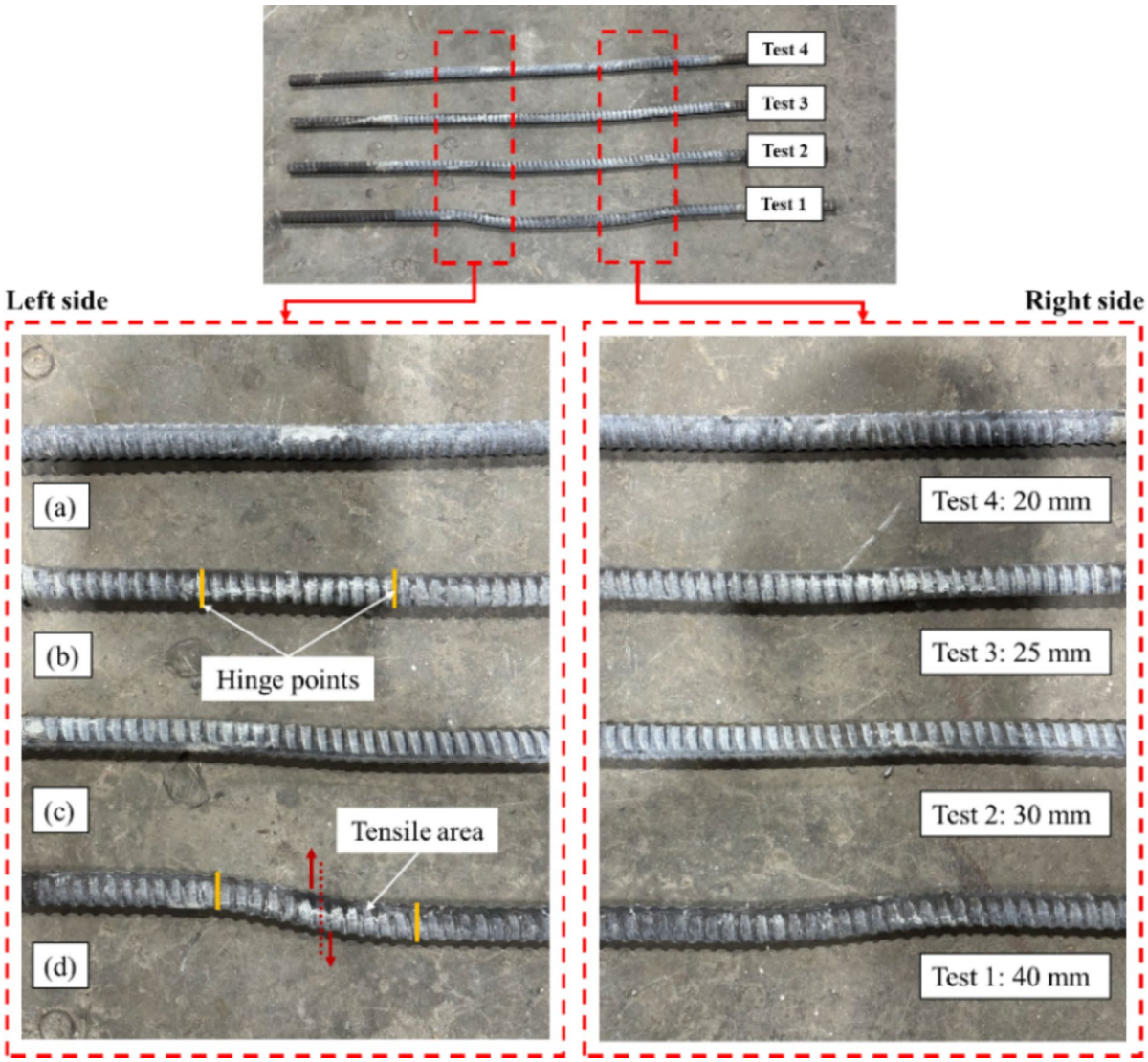

Fig. 18 Post-test conditions of the rock bolts in the DST

the surrounding host medium. The findings provide practical guidance for engineers and designers, emphasizing the need to consider specific ground conditions and loading scenarios when selecting and implementing ground reinforcement systems. Moreover, future research is needed to enhance the accuracy and repeatability of the obtained outcomes.

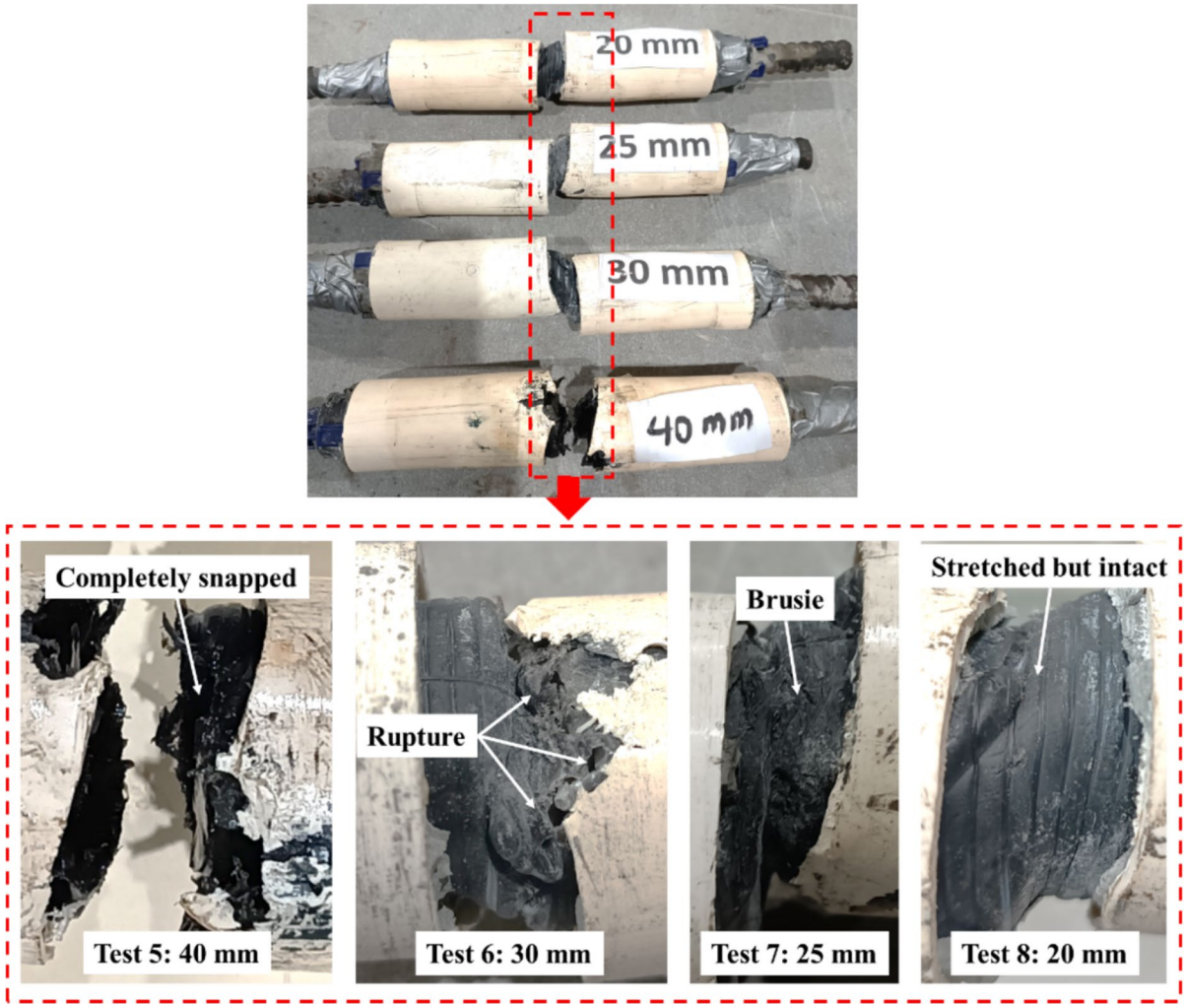

Fig. 19 The post-test observations of the SST

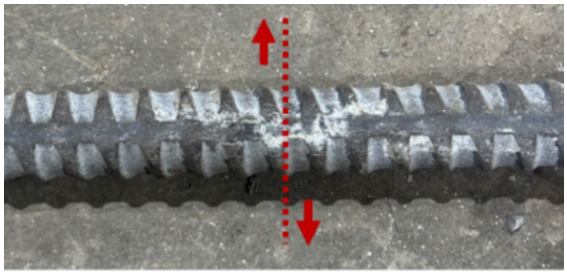

Fig. 20 The post-test condition of the rock bolt (Test 8: 20 mm displacement)

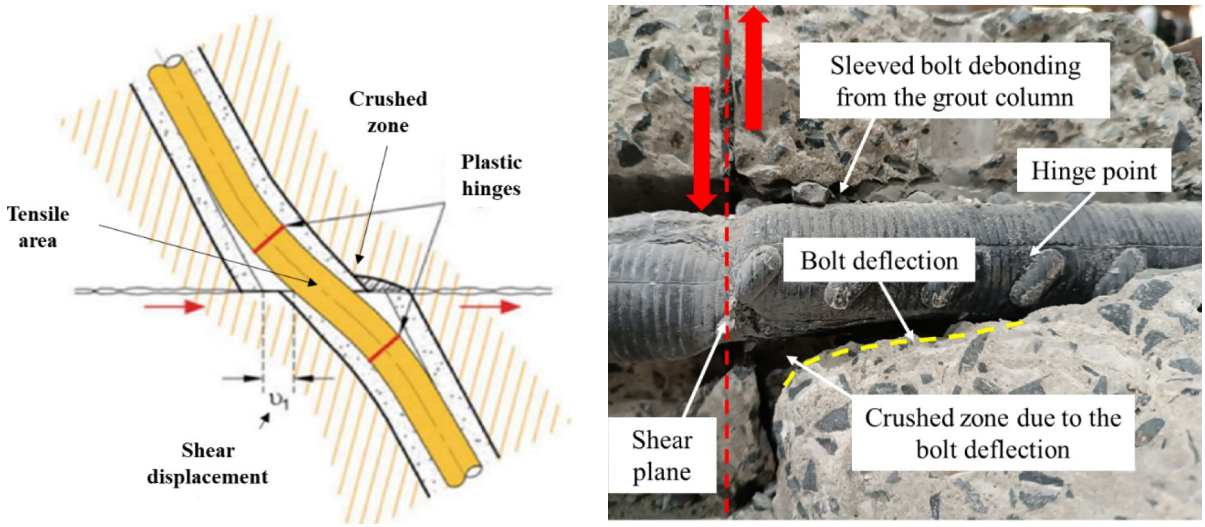

(a) Adopted from (Galvin 2016) (b) DST (Test 3)

Fig. 21 The role of the host medium in the shear loading process

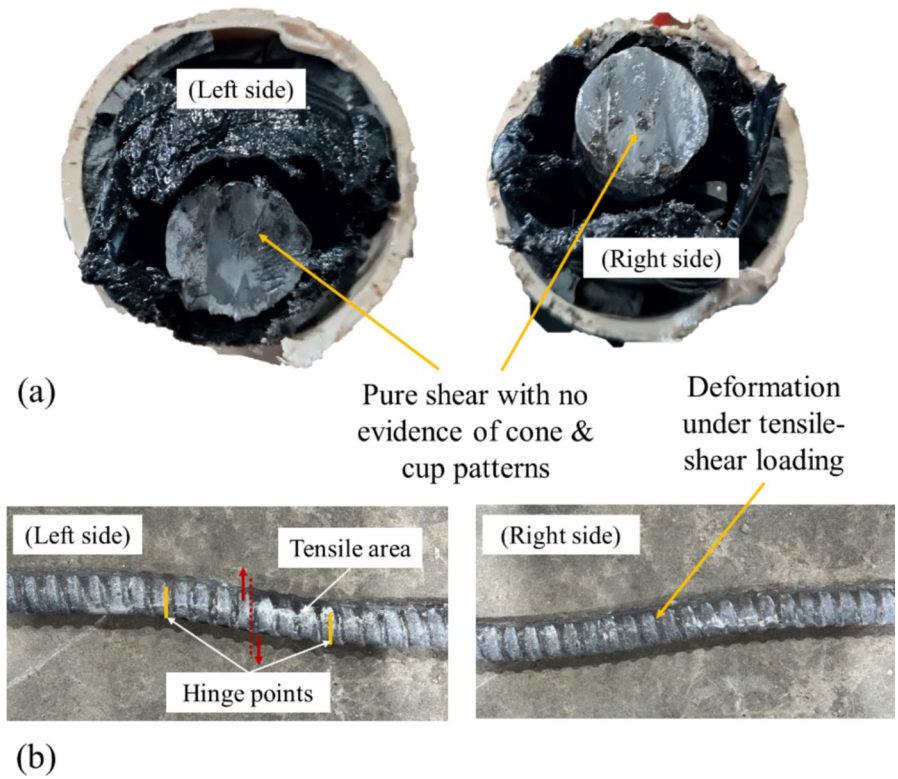

Fig. 22 The difference between failure mechanisms in the SST and DST

Acknowledgements The authors would like to express their appreciation to the university personnel who assisted in completing the tests conducted at the University of Wollongong, especially Duncan Best and Travis Marshall, and Kevin Marston verified the editorial content of the paper.

Funding Open Access funding enabled and organized by CAUL and its Member Institutions. No funding was received for conducting this study.

Data availability All data can be requested from the corresponding author.

Declarations

Conflict of interest The authors have no conflicts of interest to declare that are relevant to the content of this article.

References

Anzanpour S (2022) The load transfer mechanism of ground tendons subjected to static and dynamic loading conditions. University of Wollongong

Aziz N, Craig P, Mirzaghorbanali A, Nemcik J (2016) Factors influencing the quality of encapsulation in rock bolting. Rock Mech Rock Eng 49:3189–3203. https://doi.org/10.1007/s00603-016-0973-5

Aziz N, Pratt D, Williams R (2003) Double shear testing of bolts. In: Aziz N, Kininmonth B (eds) Proceedings of the 2003 coal operators' conference, University of Wollongong, NSW, 154–161

Aziz N, Mirzaghorbanali A, Holden M (2017) The extent of shearing and the integrity of protective sleeve coating of cable bolts. In: Aziz N, Kininmonth B (eds) Proceedings of the 2017 coal operators' conference, University of Wollongong, NSW, 240–246

Bertuzzi R (2004) 100-year design life of rock bolts and shotcrete. Ground Support in Mining and Underground Construction, London, 425–429

BS 7861–1 (2007) Strata reinforcement support system components used in coal mines. Specification for rockbolting

BS 7861–2 (2009) Strata reinforcement support systems components used in coal mines. Specification for flexible systems for roof reinforcement

Cao C, Jan N, Ren T, Naj A (2013) A study of rock bolting failure modes. Int J Min Sci Technol 23:79–88. https://doi.org/10.1016/j.ijmst.2013.01.012

Chen J, Hagan PC, Saydam S (2017) Sample diameter effect on bonding capacity of fully grouted cable bolts. Tunn Undergr Space Technol 68:238–243. https://doi.org/10.1016/j.tust.2017.06.004

Chen J, He F, Zhang S (2020) A study of the load transfer behavior of fully grouted rock bolts with analytical modelling. Int J Min Sci Technol 30:105–109. https://doi.org/10.1016/j.ijmst.2019.12.010

Chen Y, Xiao H, Huang L (2025) Analytical model for rock bolts subjected to shear load. Rock Mech Rock Eng 58:10967–10989. https://doi.org/10.1007/s00603-025-04680-9

Ding W, Huang X, Wang Z, Chen L (2022a) Experimental study on the shear performance of a prestressed anchored jointed rock-like mass under different corrosion levels. Int J Rock Mech Min Sci. https://doi.org/10.1016/j.ijrmms.2022.105209

Ding W, Wang Z, Huang X et al (2022b) Influence of corrosion on anchoring bond behavior of jointed rock mass. KSCE J Civ Eng 26:1914–1928. https://doi.org/10.1007/s12205-022-0324-x

Dywidag (2021) Dywidag Product Guide

Ferrero AM (1995) The shear strength of reinforced rock joints. Int J Rock Mech Min Sci Geomech Abstr 32:595–605. https://doi.org/10.1016/0148-9062(95)00002-X

Galvin JM (2016) Support and Reinforcement Systems. Ground engineering: principles and practices for underground coal mining. Springer, Cham, pp 211–269

Grasselli G (2005) 3d behaviour of bolted rock joints: experimental and numerical study. Int J Rock Mech Min Sci 42:13–24. https://doi.org/10.1016/j.ijrmms.2004.06.003

Gregor P, Mirzaghorbanali A, McDougall K et al (2024a) Investigating shear behaviour of fibreglass rock bolts reinforcing infilled discontinuities for various pretension loads. Can Geotech J 61:414–446. https://doi.org/10.1139/cgj-2022-0619

Gregor P, Mirzaghorbanali A, McDougall K et al (2024b) Analysing double shearing mechanism in fiberglass rock bolting systems: a comprehensive analytical model and numerical simulation approach. Geotech Geol Eng 42:7339–7370. https://doi.org/10.1007/s10706-024-02929-8

Guo C, Moore K, Vlachopoulos N (2025) Assessing cold temperature effects on fully grouted rock bolts using distributed fiber optic sensors. Geotech Geol Eng 43:135. https://doi.org/10.1007/s10706-025-03101-6

Haas CJ (1976) Shear resistance of rock bolts. Trans Soc Min Eng AIME 260:32–41

Hassell RC, Villaescusa E, Thompson AG (2006) Testing and evaluation of corrosion on cable bolt anchors. In: proceedings of the 41st U.S. rock mechanics symposium—ARMA's golden rocks 2006, 50 years of rock mechanics

He L, An XM, Zhao XB et al (2018) Development of a unified rock bolt model in discontinuous deformation analysis.

Rock Mech Rock Eng 51:827–847. https://doi.org/10.1007/s00603-017-1341-9
Høien AH, Li CC, Zhang N (2021) Pull-out and critical embedment length of grouted rebar rock bolts-mechanisms when approaching and reaching the ultimate load. Rock Mech Rock Eng 54:1431–1447. https://doi.org/10.1007/s00603-020-02318-6
Hosseini S, Jodeiri Shokri B, Mirzaghorbanali A et al (2024) Predicting axial-bearing capacity of fully grouted rock bolting systems by applying an ensemble system. Soft Comput 28:10491–10518. https://doi.org/10.1007/s00500-024-09828-3
Hutchinson DJ, Diederichs MS (1996) Cablebolting in underground mines. BiTech Publishers, Richmond, B.C
Jalalifar H, Aziz N (2010) Experimental and 3D numerical simulation of reinforced shear joints. Rock Mech Rock Eng 43:95–103. https://doi.org/10.1007/s00603-009-0031-7
Jing H-W, Yang X-X, Zhang M-L (2023) Strength and failure behaviors of a jointed rock mass anchored by steel bolts: a numerical modeling study. Geotech Geol Eng 41:225–241. https://doi.org/10.1007/s10706-022-02275-7
Knox G, Hadjigeorgiou J (2022) Shear performance of yielding self-drilling anchors under controlled conditions. In: caving 2022—fifth international conference on block and sublevel caving. Australian centre for geomechanics, Perth, 201–212
Kong C, Yang T, Xiao M, Yuan Q (2023) Numerical simulation of fully grouted rock bolts with or without faceplates based on the tri-linear bond-slip model. Constr Build Mater. https://doi.org/10.1016/j.conbuildmat.2022.130288
Li X, Aziz N, Mirzaghorbanali A, Nemcik J (2016) Behavior of fiber glass bolts, rock bolts and cable bolts in shear. Rock Mech Rock Eng 49:2723–2735. https://doi.org/10.1007/s00603-015-0907-7
Li T, Li Z, Sun J (2024) Influence of bolts and cables on stability of surrounding rock of bottom drainage roadway. Geotech Geol Eng 42:945–960. https://doi.org/10.1007/s10706-023-02597-0
Ludvig B (1984) Shear test on rock bolts. In: Balkema AA, proceedings of the international symposium on rock bolting. Rotterdam, Neth, pp 113–123
Moosavi M, Bawden WF (2003) Shear strength of Portland cement grout. Cem Concr Compos 25:729–735. https://doi.org/10.1016/S0958-9465(02)00101-4
Moosavi M, Jafari A, Khosravi A (2005) Bond of cement grouted reinforcing bars under constant radial pressure. Cem Concr Compos 27:103–109. https://doi.org/10.1016/j.cemconcomp.2003.12.002
Mottahedi A, Aziz N, Remennikov A et al (2025) A critical review on development of laboratory testing technologies of tendons applied to stabilize underground structures. Rock Mech Rock Eng. https://doi.org/10.1007/s00603-025-04518-4
Nourizadeh H, Mirzaghorbanali A, McDougall K et al (2023) Characterization of mechanical and bonding properties of anchoring resins under elevated temperature. Int J Rock Mech Min Sci. https://doi.org/10.1016/j.ijrmms.2023.105506
Nourizadeh H, Mirzaghorbanali A, Serati M et al (2024) Failure characterization of fully grouted rock bolts under triaxial testing. J Rock Mech Geotech Eng 16:778–789. https://doi.org/10.1016/j.jrmge.2023.08.013
Nourizadeh H, Mirzaghorbanali A, McDougall K et al (2025a) Unveiling axial load transfer mechanism in fully encapsulated rock bolts. Rock Mech Rock Eng 58:4043–4067. https://doi.org/10.1007/s00603-024-04347-x
Nourizadeh H, Mirzaghorbanali A, McDougall K, Aziz N (2025b) Exploring the axial performance of protective sheathed rock bolts through large-scale testing. Tunn Undergr Space Technol 155:106157. https://doi.org/10.1016/j.tust.2024.106157
Peter K, Moshood O, Akinseye PO et al (2022) An overview of the use of rockbolts as support tools in mining operations. Geotech Geol Eng 40:1637–1661. https://doi.org/10.1007/s10706-021-02005-5
Rastegarmanesh A, Mirzaghorbanali A, McDougall K et al (2025) Performance of cable bolts in small- and large-scale laboratory pullout tests. Geotech Geol Eng 43:67. https://doi.org/10.1007/s10706-024-03019-5
Satola I, Hakala M (2001) Corrosion protected cable bolts in long-term reinforcement. Balkema, Rotterdam, Neth, pp 377–382
Thirukumaran S, Oliveira D, Ariza L (2025) Assessing the relative quality of rock bolt grouting in weak rock mass based on in situ and numerical pull-out tests. Rock Mech Rock Eng 58:10497–10522. https://doi.org/10.1007/s00603-025-04647-w
Thompson AG, Villaescusa E, Windsor CR (2012) Ground support terminology and classification: an update. Geotech Geol Eng 30:553–580. https://doi.org/10.1007/s10706-012-9495-4
Villaescusa E, Windsor CR (1999) Reinforcement of underground excavations using the CT Bolt. In: Thompson AG (ed) Rock Support and Reinforcement Practice in Mining. Routledge, London, UK
Wu S, Chen H, Lamei Ramandi H et al (2018) Investigation of cable bolts for stress corrosion cracking failure. Constr Build Mater 187:1224–1231. https://doi.org/10.1016/j.conbuildmat.2018.08.066
Zhao D, Wen S, Wang L et al (2021) Structural parameters and critical anchorage length of tunnel system bolts made of basalt fibre. Constr Build Mater. https://doi.org/10.1016/j.conbuildmat.2021.125081
Zheng H, Wu X, Jiang Y et al (2024) Shear behavior of rock joints reinforced with fully-grouted and energy-absorbing bolts subjected to shear cycles. J Rock Mech Geotech Eng. https://doi.org/10.1016/j.jrmge.2024.09.056